Proton ionizable 1*H*-1,2,4-triazole π-electron deficient cyclophanes as hosts and in [2]catenanes†‡

Susana Ramos,[a] Ermitas Alcalde,[a] J. Fraser Stoddart,[b] Andrew J. P. White,[c] David J. Williams*[c] and Lluïsa Pérez-García*[a]

Received (in Montpellier, France) 3rd September 2008, Accepted 5th November 2008
First published as an Advance Article on the web 19th December 2008
DOI: 10.1039/b815355h

The incorporation of proton ionizable moieties, such as 1*H*-1,2,4-triazole rings, within cyclophanes and π-donor/π-acceptor [2]catenanes is explored as a tool of inducing chemical switchability through either the inherent prototropic tautomerism or chemical deprotonation. Bearing this in mind, in this paper we describe the template-directed synthesis of two tetracationic cyclophanes incorporating two bipyridinium units linked by either *one* 3,5-bis(methylene)-1*H*-1,2,4-triazole unit and a *p*-xylyl unit or *two* 3,5-bis(methylene)-1*H*-1,2,4-triazole units, as well as the template-directed synthesis of two [2]catenanes wherein these π-acceptor cyclophanes are interlocked with (bis-*p*-phenylene-34-crown-10), as the π-electron rich polyether macrocycle. We also report on the full characterization of the cyclophanes and the [2]catenanes by electrospray mass spectrometry (ESMS) and fast atom bombardment mass spectrometry (FABMS), X-ray crystallography of the [2]catenanes and dynamic ^{1}H NMR spectroscopy. We reveal that the [2]catenane incorporating one triazole ring in the tetracationic cyclophane exists, in the solid-state, as hydrogen bond cross-linked enantiomeric pair stacks, whereas the [2]catenane incorporating two triazole rings in the tetracationic cyclophane does not form polar stacks, unlike most of the [2]catenanes of this class. Finally, we studied the chemical stability of these π-donor/π-acceptor motifs to explore their chemical switchability, to show the triazolate–bipyridinium pair is a challenging one in this sense.

Introduction

Ever since Sauvage and Dietrich-Buchecker showed that catenanes could be produced in large amounts[1] using template strategies,[2] these and related molecular architectures[3] have been turned from chemical curiosities into key components in the fabrication of nanoscale devices.[4] A particularly fruitful combination of templates is the π–donor/π–acceptor system developed by Stoddart,[5] a relevant approach to the field of molecular switches.[6]

This latter family of catenanes and rotaxanes are interlocked molecules whose components exhibit dynamic behaviour in solution.[7] Different properties have been explored to induce directionality to their motion, but to the best of our knowledge, prototropic tautomerism has not yet been used for this purpose. Following the previous experience of our research group,[8,9] we have been interested in the incorpora;tion of proton ionisable heteroaromatic systems, *e.g.* 1*H*-1,2,4-triazole units[8] into mechanically interlocked structures, and we described[10] the synthesis of two [2]catenanes which incorporate the tetracationic cyclophane cyclobis(paraquat-*p*-phenylene) as the -electron deficient component and a macrocyclic polyether as the π-electron rich component incorporating either *one* 1,4-dioxybenzene or 1,5-dioxynaphthalene ring and *one* 3,5-bis(oxymethylene)-1*H*-1,2,4-triazole unit, and both [2]catenanes exhibited spontaneous resolution upon crystallization.

With this backdrop, in this work we have explored the incorporation of 1*H*-1,2,4-triazole subunits within tetracationic cyclophanes and used these rings as components of [2]catenanes (see structural formulae below), and have studied the influence on their properties induced by these heteroaromatic moieties.

Here, we describe the synthesis of the [2]catenanes **10**·4PF$_6$ and **11**·4PF$_6$, which incorporate the macrocyclic polyether **8** (bis-*p*-phenylene-34-crown-10), as the π-electron rich component, and a tetracationic cyclophane as the π-electron deficient component incorporating two bipyridinium units linked by either *one* 3,5-bis(methylene)-1*H*-1,2,4-triazole unit and a *p*-xylyl unit or *two* 3,5-bis(methylene)-1*H*-1,2,4-triazole units, as well as the preparation of their tetracationic cyclophane components **6**·4PF$_6$ and **7**·4PF$_6$, respectively. We report the characterization of **6**·4PF$_6$, **7**·4PF$_6$, **10**·4PF$_6$ and **11**·4PF$_6$ by electrospray (ESIMS) and fast atom bombardment mass spectrometry (FABMS), X-ray crystallography, and dynamic

[a] *Laboratory of Organic Chemistry, Faculty of Pharmacy and Institute of Nanoscience and Nanotechnology (IN^{2}UB), University of Barcelona, Avda. Joan XXIII s/n, Barcelona, 08028, Spain. E-mail: mlperez@ub.edu; Fax: +34 93-4024539*
[b] *Department of Chemistry, Northwestern University, Evanston, IL 60208, USA. E-mail: stoddart@northwestern.edu; Fax: +1 847-491-1009*
[c] *Department of Chemistry, Imperial College, South Kensington, London, UK SW7 2AY. E-mail: d.williams01@ic.ac.uk; Fax: +44 171-594-5804*

† Dedicated to Professor Jean-Pierre Sauvage on the occasion of his 65th birthday.

‡ CCDC reference numbers 708196 and 708197. For crystallographic data in CIF or other electronic format see DOI: 10.1039/b815355h

^{1}H NMR spectroscopy. In order to explore the chemical switchability of the proton ionisable 1*H*-1,2,4-triazole moieties, some simple model compounds incorporating pyridinium or bipyridinium and 1*H*-1,2,4-triazole units, **13**·PF_6, **14**·$2PF_6$ and **15**·$4PF_6$, were prepared. Their ability to bind π-electron rich components, such as **8**, and their stability under basic conditions was explored.

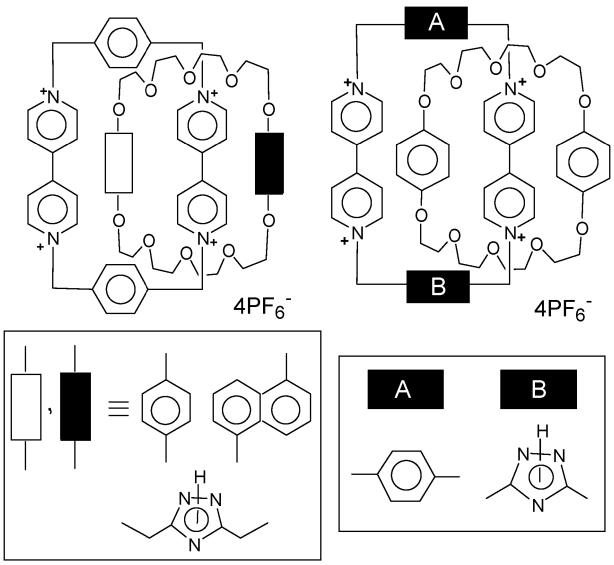

Structural formulae

Results and discussion

Synthesis

Preparation of tetracationic cyclophane **6**·$4PF_6$ was achieved by two procedures (Chart 1). Following route A, by reaction of 1,1′-[1,4-phenylenebis(methylene)]bis-4,4′-pyridylpyridinium **1**·$2PF_6$[11] with 3,5-bis(chloromethyl)-1*H*-1,2,4-triazole **3**[8] in DMF under high pressure conditions (10 kbar), after purification and anion exchange (NH_4PF_6/H_2O), cyclophane **6**·$4PF_6$ was obtained in 2% yield. Route B relies on using a template directed methodology. Thus, reaction of 1,1′-[1*H*-1,2,4-triazolo-3,5-bis(methylene)]bis-4,4′-pyridylpyridinium **2**·$2PF_6$—previously prepared by reaction of 4,4'-bipyridine and 3,5-bis(chloromethyl)-1*H*-1,2,4-triazole **3**[8]—with 1,4-bis(bromomethyl)benzene **4** in the presence of 1,4-bis[2-(2-hydroxyethoxy)ethoxy]benzene **5**,[11] under high pressure conditions (10 kbar) afforded a complex between the tetracationic cyclophane and **5**. Decomplexation by column chromatography gave the cyclophane **6**·$4PF_6$ in 13% yield after counterion exchange (Chart 1). Increasing the pressure to 13 kbar induced a slight improvement of the yield of **6**·$4PF_6$ to 15% (Chart 1).

Following route B, synthesis of the tetracationic cyclophane **7**·$4PF_6$ was also achieved (Chart 1). By reaction of precursor **2**·$2PF_6$ with 3,5-bis(chloromethyl)-1*H*-1,2,4-triazole **3**,[8] using **5** as template in DMF and under high pressure conditions (10 kbar), after decomplexation and counterion exchange, the cyclophane **7**·$4PF_6$ was obtained in 1% yield, whereas the yield was improved up to 3.5% by raising the pressure to 13 kbar.

The [2]catenanes **10**·$4PF_6$ and **11**·$4PF_6$ were prepared using a template-directed methodology (Chart 2 and Chart 3). Two approaches were compared for the [2]catenane **10**·$4PF_6$ (Chart 2). Reaction of **1**·$2PF_6$[11] and **3**[8] in the presence of the appropriate macrocyclic polyether **8**[11] generated a tricationic intermediate, which leads to the [2]catenane **10**·$4PF_6$ after macrocyclization. When the reaction was carried out in DMF, using sodium iodide for halogen exchange, the yield of the [2]catenane **10**·$4PF_6$ was 1% after 17 days, whereas under high pressure conditions (10 kbar), it was obtained in 6% yield after counterion exchange (Chart 2). On the other hand, reaction of **2**·$2PF_6$[11] and 1,4-bis(chloromethyl)benzene **9**—used to make both routes comparable—in the presence of the macrocyclic polyether **8**[11] under high pressure conditions (10 kbar) gave the [2]catenane **10**·$4PF_6$ in 14% yield (Chart 2). Clearly, these yields indicate that this route proceeds through a tricationic intermediate with a more favoured geometry for the ring closure leading to **10**·$4PF_6$.

The [2]catenane **11**·$4PF_6$ was prepared by reaction of **2**·$2PF_6$ and the triazole **3**[8] in the presence of the macrocyclic polyether **8**[11] under high pressure conditions (10 kbar) and it was obtained in 1% yield (Chart 3). Furthermore, increasing the pressure to 13 kbar, resulted in a significant increase to 5% yield of the [2]catenane **11**·$4PF_6$ (Chart 3).

The experimental conditions and yields for the preparation of compounds **6**·$4PF_6$, **7**·$4PF_6$, **10**·$4PF_6$ and **11**·$4PF_6$ are indicated in Table 1. The low yields obtained can be explained by two facts: (a) the use of the chloro derivatives (**3** or **9**) as reagents for the ring closure step of the tricationic intermediate, instead of more reactive bromo derivatives§ and (b) the geometry of the tetracationic cyclophanes incorporating 1,2,4-triazole rings as spacers between the bipyridinium units, also with smaller cavities (see later, crystallographic study) resulting in a less efficient self-assembly process.¶

Preparation of the quaternary salt **13**·PF_6 was achieved by slow addition of 3(5)-chloromethyl-1*H*-1,2,4-triazole **12**[14] over an excess of 4,4′-bipyridine followed by counteranion exchange (Chart 4). Instead, reaction of 4,4′-bipyridine with 2 equivalents of the triazole **12** yielded the salt **14**·$2PF_6$. Compound **15**·$4PF_6$ was synthesized by reaction of **2**·$2PF_6$ with benzyl bromide (Chart 4). Treatment of quaternary salt **13**·PF_6 with a strongly basic anion-exchange resin (AER-hydroxide form) gave the corresponding betaine **16**, together with decomposition products, whereas the salts **14**·$2PF_6$ and **15**·$4PF_6$, under the same conditions, did not afford the corresponding betaines **17** and **18**, due to their high instability (Chart 4).‖

The yields for the synthesis of cyclophanes and [2]catenanes incorporating 1*H*-1,2,4-triazole rings are relatively low in

§ 3,5-Bis(bromomethyl)-1*H*-1,2,4-triazole could not be prepared due to its instability.[12]

¶ Using a similar procedure, the tetracationic cyclophane incorporating two *p*-xylyl spacers could be obtained in 62% yield,[11] whereas the cyclophane containing one *p*-xylyl and one *m*-xylyl formed only in about 7%.[13]

‖ The high instability of these triazolate bipyridinium inner salts is consistent with previously obtained results in 1,2,4-triazolate-, pyrazolate- and benzimidazolate-pyridinium betaines previously described.[14]

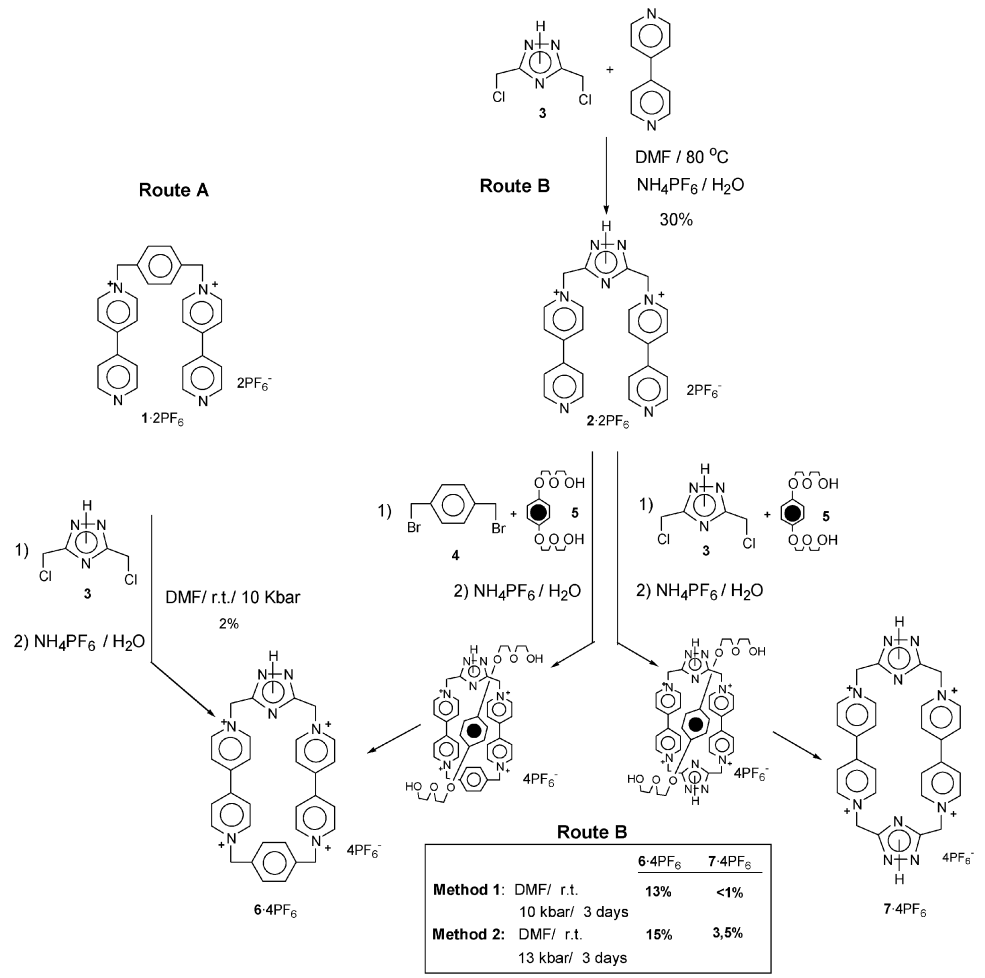

Chart 1

general, although they can be slightly improved by the use of high-pressure conditions, the reason being related to the geometries and dimensions of these π-electron deficient systems (see later, X-ray crystallography).

Mass spectrometry

In both cases, the structure of the [2]catenanes **10**·4PF_6 and **11**·4PF_6 was characterized by positive-ion FABMS, revealing singly charged ions characteristic of the successive loss of one, two, three and four PF_6^- counterions from the molecular ion (Table 2). An additional doubly charged ion corresponding to the dicationic fragment after the loss of two counterions is also observed $([M + 2PF_6]/2)^{2+}$. Peaks corresponding to the loss of two and three PF_6^- counterions from the free cyclophane component of the [2]catenanes are also characteristic of the fragmentation of the [2]catenane after loss of the neutral crown ether component (Table 2).

The positive ion ESI-MS of the tetracationic cyclophane **6**·4PF_6 reveals peaks characteristic of the successive loss of two, three and four PF_6^- counterions from the molecular ion (Table 2). Instead, for cyclophane **7**·4PF_6 only the doubly charged ion corresponding to the dicationic fragment after the loss of two counterions is observed $([M + 2PF_6]/2)^{2+}$ as the most abundant fragment. Singly charged ions characteristic of the successive loss of one and two PF_6^- counterions from the molecular ion are also observed for both cyclophanes (Table 2).

For dicationic precursor **2**·4PF_6, ESI-MS singly charged ions are observed, corresponding to the loss of one and two PF_6^- counterions from the molecular ion (Table 2).

X-Ray crystallography

Both catenanes provided single crystals suitable for X-ray crystallography when grown by vapor diffusion of *i*-Pr_2O into MeCN solutions of **10**·4PF_6 and **11**·4PF_6.

The X-ray analysis of **10**·4PF_6 shows the molecule to have a co-conformation very reminiscent of the [2]catenane formed between BPP34C10 and cyclobis(paraquat-*para*-phenylene),[11] the tetracation encircling one of the hydroquinone residues of the crown ether macrocycle (Fig. 1). The only major difference accompanying the replacement of one of the *p*-xylyl spacers by a 3,5-dimethylene-1*H*-1,2,4-triazole unit is the adoption of an *anti*-geometry for the oxymethylene groups attached to the alongside hydroquinone ring system, *cf.* a *syn* geometry in the original [2]catenane,[11] (the conformation of one of the poly-ether loops is essentially unchanged), and a shortening of the methylene···methylene separation in the shorter arm of the tetracation from *ca.* 5.8 to 5.0 Å. A consequence of this

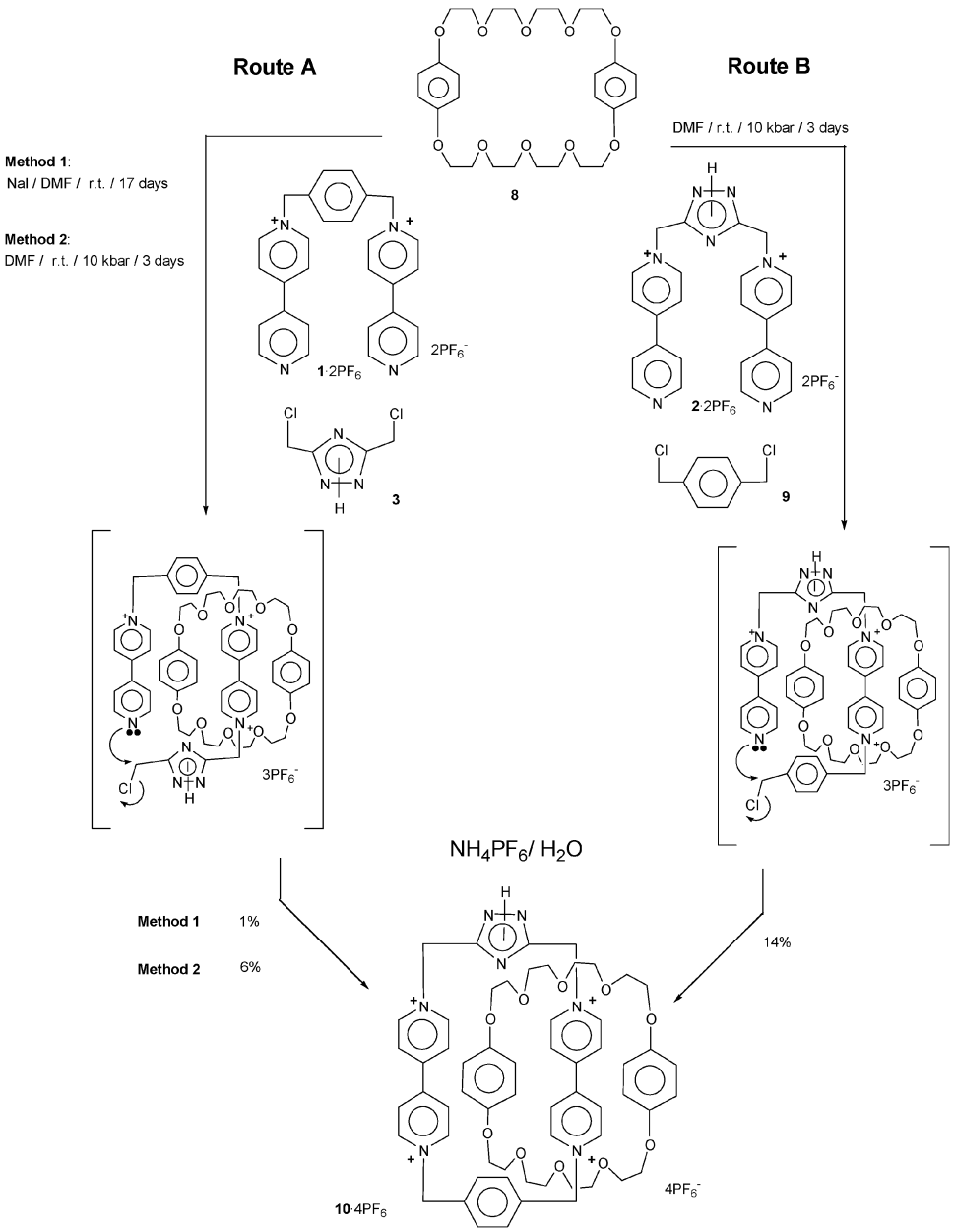

Chart 2

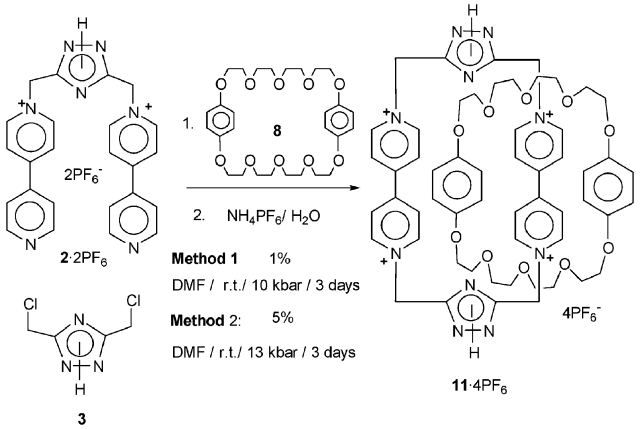

Chart 3

contraction within the tetracation is a reduction of the separation, by *ca.* 0.1 Å, between the inside hydroquinone residue and the two bipyridinium ring systems, and a significant increase in the "bowing" of the bipyridinium residues (Table 3); the internal angles at the four methylene carbon atoms are also enlarged. The tilt of the O···O vector of the inside O–C_6H_4–O unit to the plane of the tetracation is *ca.* 44°. The alongside hydroquinone ring system is displaced laterally such that it lies more over the pyridinium ring system proximal to the triazole ring *cf.* being essentially centrally positioned over the bipyridinium unit in the original [2]catenane.[11] In addition to the π–π interactions between the π-electron rich hydroquinone residues and the π-electron deficient bipyridinium ring systems, the [2]catenane is stabilised by weak hydrogen bonding. These include (a) an N–H···O hydrogen bond between the triazole ring N–H group and the central oxygen

Table 1 Experimental conditions for the formations of the tetracationic cyclophanes **6**·4PF_6, **7**·4PF_6 and the [2]catenanes **10**·4PF_6 and **11**·4PF_6

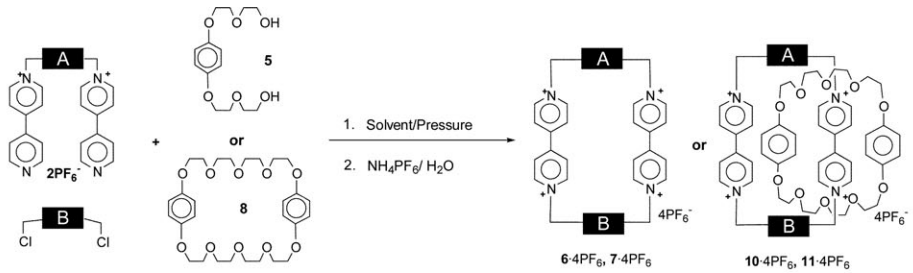

		A	B	Solvent	Pressure (Kbar)	Template	Yield (%)
Tetracationic cyclophanes	**6**·4PF_6			DMF	10	none	**2**
			[a]	DMF	10	**5**	**13**
					13	**5**	**15**
	7·4PF_6			DMF	10	**5**	**<1**
					13	**5**	**3,5**
[2]Catenanes	**10**·4PF_6			DMF	Ambient	**8**	**1**
					10	**8**	**6**
				DMF	10	**8**	**14**
	11·4PF_6			DMF	10	**8**	**1**
					13	**8**	**5**

[a]Using 1,4-bis(bromomethyl)benzene **4**.

atom of one of the polyether loops, (b) a C–H···O linkage between one of the α-pyridinium hydrogen atoms and the central oxygen atom of the opposite polyether loop, (c) a C–H···π interaction between one of the C–H groups of the inside hydroquinone ring and the *p*-xylyl ring in the tetracation and (d) a C–H···N(pπ) interaction[15] between the opposite hydroquinone C–H group and the inwardly directed triazole nitrogen atom N-4 (the H···triazole ring centre distance, and the geometry of approach, preclude any possible C–H···π interaction). This latter interaction is facilitated by a noticeable tilting of the triazole ring system such that the apical nitrogen atom is directed into the cyclophane ring centre (the triazole ring is inclined by 76° to the mean plane of the cyclophane—as defined by the four corner methylene carbon atoms—whereas the *p*-xylyl ring is aligned almost orthogonally, *ca.* 87°, to this plane).

The molecules pack to form continuous π-donor···π-acceptor polar stacks (Fig. 2A) directly analogous to those seen in the structure of the original [2]catenane, the alongside hydroquinone unit of one molecule being positioned in a π-stacking relationship with one of the pyridinium rings (that adjacent to the *p*-xylyl spacer) of the alongside bipyridinium moiety of a lattice translated (in *a*) counterpart, the mean interplanar separation being *ca.* 3.34 Å. Adjacent, centrosymmetrically related, enantiomeric stacks are cross-linked by pairs of C–H···N hydrogen bonds between one of the α-C–H groups of the alongside pyridinium ring proximal to the triazole ring in one molecule and the apical nitrogen N-4 of the triazole ring of the next and *vice versa* (Fig. 2B). These enantiomeric stacks are linked to their neighbours by a weak parallel π–π stacking interaction between their *p*-xylyl ring systems, the centroid···centroid and mean interplanar separations being 4.35 and 3.29 Å, respectively. Of the four PF_6 anions, only one is ordered and this is positioned over the edge of the alongside bipyridinium unit; the shortest C–H···F contact is from a β-pyridinium hydrogen atom having C···F and H···F distances of 3.38 and 2.45 Å, respectively, with a C–H···F angle of 164°.

The solid-state structure of the [2]catenane **11**·4PF_6 reveals that replacement of both *p*-xylyl spacers within the tetracation in the original [2]catenane by 3,5-dimethylene-1*H*-1,2,4-triazole units results in a pseudo-centrosymmetric geometry for the tetracationic cyclophane (Fig. 3) and a further reduction of *ca.* 0.1 Å in the separation of the inside hydroquinone ring and the sandwiching bipyridinium ring systems within the [2]catenane from that seen in **10**·4PF_6 (Table 3). The geometry of the BPP34C10 macrocycle is different from that observed in **10**·4PF_6 with the inside and alongside CH_2–O–C_6H_4–O–CH_2 units having *anti* and *syn* geometries for their respective oxymethylene groups *cf.* an *anti–anti* relationship in **10**·4PF_6. The "bowing" of the alongside bipyridinium unit is increased significantly from that seen in **10**·4PF_6, whereas in the inside unit it is slightly reduced (Table 3). As in **10**·4PF_6, the alongside hydroquinone ring is displaced so as to lie more over one pyridinium ring than the other. The tilt of the inside O–C_6H_4–O axis to the mean plane of the tetracation cyclophane is increased slightly to *ca.* 45°. The planes of the two

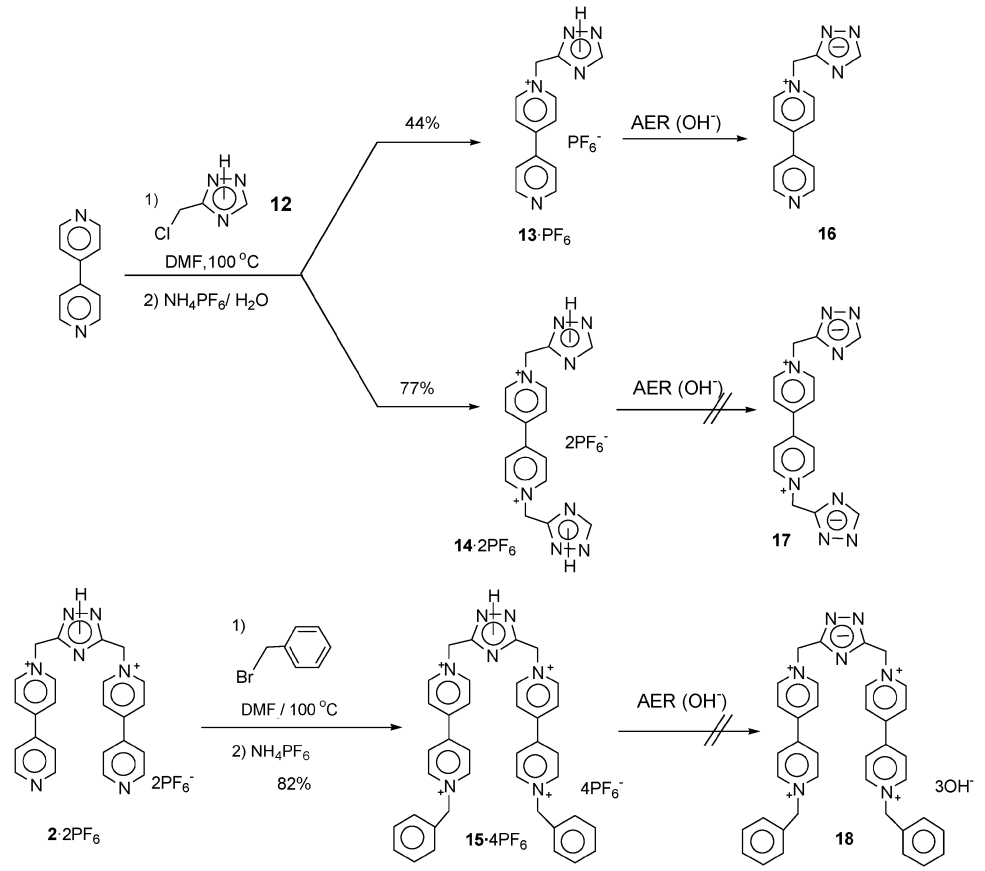

Chart 4

Table 2 Positive ESI-MS[a] data for compound **2**·2PF_6, cyclophanes **6**·4PF_6, **7**·4PF_6 and FAB-MS[b] data for the [2]catenanes **10**·4PF_6 and **11**·4PF_6

	m/*z*								
	Relative abundance (%)								
Compd (MW)	$[M + 3PF_6]^+$	$[M + 2PF_6]^+$	$[M + PF_6]^+$	$[M]^+$	$[M + 2PF_6 - EC^d]^+$	$[M + PF_6 - EC^d]^+$	$[M + 2PF_6/2]^{2+}$	$[M + PF_6/3]^{3+}$	$[M/4]^{4+}$
2·2PF_6	552.2	203.6	—	—	—	—	—	—	—
(697.5)	(**100**)	(36)							
6·4PF_6	947.7	801.1	[c]	[c]	—	—	400.9	218.7	128.1
(1091.0)	(5)	(2)					(**100**)	(2)	(1)
7·4PF_6	937.2	791.9	[c]	[c]	—	—	396.2	[c]	[c]
(1082.4)	(11)	(3)					(**100**)		
10·4PF_6	1482.5	1337.8	1192.9	1047.1	800.6	656.6	669.2	[c]	[c]
(1628.2)	(4)	(26)	(23)	(10)	(30)	(**100**)	(23)		
11·4PF_6	[c]	1331.1	1184.2	1037.9	792.0	647.0	665.1	[c]	[c]
(1618.2)		(51)	(58)	(35)	(43)	(**100**)	(46)		

[a] ESI-MS in positive mode. Solvent H_2O–CH_3CN (1 : 1, v/v) and Focus Voltage 60 V. [b] FAB-MS in positive mode. Matrix NBA. [c] Not observed. [d] EC: macrocyclic polyether.

triazole rings are inclined by 66 and 79° to the mean plane of the tetracation. This inclination facilitates the formation of an intra[2]catenane N–H···O hydrogen bond between the 1*H* N–H hydrogen atom of one of the triazole rings and the central oxygen atom of its proximal polyether loop (a in Fig. 3), an interaction directly analogous to that seen in **10**·4PF_6. The N–H hydrogen atom of the other triazole ring is directed away from its adjacent polyether loop and forms a weak N–H···N hydrogen bond with one of the included acetonitrile solvent molecules (N···N, H···N 3.03, 2.39 Å, N–H···N 129°). Other intra[2]catenane interactions include (b) a C–H···O hydrogen bond between one of the α-pyridinium hydrogen atoms of the inside bipyridinium unit and the second oxygen atom (from the inside hydroquinone ring) of one of the polyether loops, and (c) & (d) a pair of C–H···N(pπ) contacts analogous to interaction (d) in **10**·4PF_6.

By contrast with the majority of related [2]catenanes studied previously, **11**·4PF_6 does not form polar stacks, and in fact

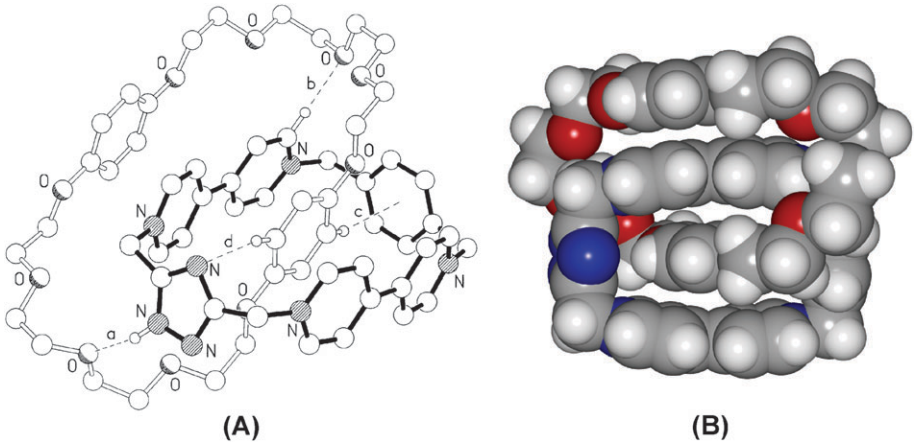

Fig. 1 The molecular structure of **10**·4PF$_6$ showing the intra[2]catenane hydrogen bonding interactions. The hydrogen bonding geometries are (a) N···O, H···O (Å), N–H···O (°), 2.76, 1.88, 165; (b) C···O, H···O (Å), C–H···O (°), 3.30, 2.42, 152; (c) H···π (Å), C–H···π (°), 2.77, 162; (d) C···N, H···N (Å), C–H···N (°), 3.53, 2.59, 165; (A) Lateral view (B), CPK model.

there are no inter[2]catenane interactions of note, probably because the incorporation of the triazole ring disturbs the symmetry of the cyclophane within the [2]catenane. Of the four PF_6 anions, three are ordered and are positioned over the edges of either the inside or alongside bipyridinium units. These ordered anions are each involved in hydrogen bonding with β-pyridinium hydrogen atoms with the shortest C···F contacts having C···F, H···F (Å), C–H···F (°) geometries of 3.30, 2.36, 169; 3.33, 2.38, 169 and 3.32, 2.37, 173 to fluorine atoms in the three PF_6 anions, respectively.

The structure of both [2]catenanes **10**·4PF$_6$ and **11**·4PF$_6$ has been confirmed by X-ray crystallography, which shows intra- and intermolecular interactions. Particularly noteworthy is the presence in the solid state of only one isomer for the [2]catenane **11**·4PF$_6$, with the two triazole hydrogen atoms in a *transoid* disposition within the [2]catenane.

Dynamic NMR spectroscopy

The full assignment of the NMR signals, for both the tetracationic cyclophanes and the macrocyclic polyether, was achieved with help from the previous studies on [2]catenanes.[11] Furthermore unambiguous assignments have been possible by using HMBC, HMQC, COSY-2D and ROESY-2D techniques, and the results are collected in Table 4 for the tetracationic cyclophanes **6**·4PF$_6$ and **7**·4PF$_6$ and for the [2]catenanes **10**·4PF$_6$ and **11**·4PF$_6$ (Table 4).

In order to explore the prototropic tautomerism of the 1*H*-1,2,4-triazole unit, we studied the tetracationic cyclophane **6**·4PF$_6$. The ^{1}H NMR spectrum of **6**·4PF$_6$, recorded in CD_3COCD_3 solution at room temperature, indicates a fast exchange of the hydrogen atom on the 1,2,4-triazole unit, as indicated by the presence of only *one* sharp singlet at δ 6.33 ppm for the methylene groups linked to this ring (Fig. 4(a)). By cooling down the solution to 233 K, the tautomerism slows down, as indicated by the broadening of the methylene signal (Fig. 4(b)), and at 198 K two different singlets of equal intensity appear at δ 6.25 ppm and δ 6.55 ppm (Fig. 4(c)). By following the coalescence of this peak, the energy associated to the process could be calculated ($\Delta G^{\ddagger}$ = 45.19 kJ mol^{-1}) (Table 5).

For the tetracationic cyclophane **7**·4PF$_6$, the prototropic tautomerism could also be evaluated ($\Delta G^{\ddagger}$ = 43.51 kJ mol^{-1}) (Table 5) by following the coalescence of the methylene hydrogen atoms linked to the 1,2,4-triazole unit, which evolves from a singlet at room temperature, δ 6.40 ppm (Fig. 5(a)), to a broad signal at 224 K (Fig. 5(b)) to a two signals (δ 6.27 and 6.57) at 198 K (Fig. 5(c)). In this case, the formation of two different isomers, in proportion *ca.* 2 : 1 could be detected, as indicated by the presence of another set of two signals for the methylene protons. The presence of these isomers is a consequence of the prototropic tautomerism operating in **7**·4PF$_6$, with *cisoid* and *transoid* dispositions being possible for the hydrogen atoms of the triazole rings in the cyclophane.

The [2]catenanes **10**·4PF$_6$ and **11**·4PF$_6$ exhibit dynamic behaviour in solution, observed by NMR, consequence of a number of dynamic processes, as described for similar compounds,[11] and shown in Chart 5.

The ^{1}H NMR spectrum of **10**·4PF$_6$, recorded in CD_3CN solution at room temperature, shows that circumrotation of the macrocyclic polyether through the cavity of the tetracationic cyclophane (process I) is not occurring, with no exchange of the 1,4-dioxybenzene rings between the inside and alongside positions on the NMR timescale. This statement is based on the chemical shift values for the only *one* signal corresponding to the 1,4-dioxybenzene ring alongside the tetracation cavity (δ 6.21 ppm) and the only *one* signal corresponding to the 1,4-dioxybenzene ring inside the tetracation cavity (δ 3.95 ppm), exhibiting a upfield shift of $\Delta\delta$ = −2.81 ppm referred to the values for the aromatic rings of the free component **8** (Fig. 6(a), Table 4). There is further evidence based on two observations, (a) warming the CD_3CN solution up to 323 K (Fig. 6(b)) and to 343 K (Fig. 6(c)) showed broadening for the aromatic hydrogen of the 1,4-dioxybenzene rings, indicating a slow exchange, (b) by cooling down to 203 K a CD_3COCD_3 solution of **10**·4PF$_6$, the chemical shift of these protons do not experience any significant variation (Fig. 7, see below).

The ^{1}H NMR spectrum of **10**·4PF$_6$, recorded in CD_3COCD_3 solution is very similar to the one recorded in CD_3CN solution at room temperature, with no circumrotation

Table 3 Structural parameters for the [2]catenanes **10**·4PF$_6$ and **11**·4PF$_6$[a]

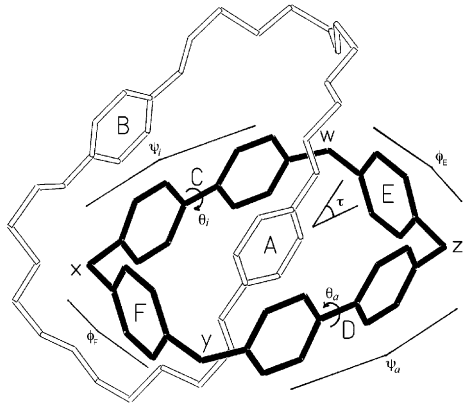

Data	**10**·4PF$_6$[b]	**11**·4PF$_6$[c]
θ_i[d]/°	9	11
θ_e[d]/°	4	4
ψ_i[e]/°	29	28
ψ_e[e]/°	29	33
ϕ_E[f]/°	11	3
ϕ_F[f]/°	3	0
τ[g]/°	44	45
A···B/Å	6.68	6.54
C···D/Å	6.82	6.63
E···F/Å	10.22	10.40
A···C/Å	3.41	3.29
A···D/Å	3.42	3.34
C···B/Å	3.46	3.32
A···E/Å	5.05	5.16
A···F/Å	5.22	5.24
w/°	108.9(3)	110.2(3)
x/°	110.0(3)	109.1(2)
y/°	110.5(3)	110.5(3)
z/°	108.4(3)	110.4(3)

[a] For the angles θ and ψ, the subscripts 'i' and 'a' refer to the *inside* and *alongside* ring systems respectively. Distances to the rings systems A to F are calculated from centroid to centroid. [b] Ring E is *p*-phenyl and ring F is 3,5-substituted-1*H*-1,2,4-triazole. [c] Rings E and F are both 3,5-substitued-1*H*-1,2,4-triazoles. [d] The twist angle θ is defined as the average of the moduli of the four normalised torsional angles about the central C–C bond within the bipyridinium unit. [e] The bowing angle ψ is the supplement of the angle subtended by the two N^+–CH_2 bonds emanating from the bipyridinium ring system. [f] The bowing angle ϕ is the supplement of the sum of the angles of the C–CH_2 bonds emanating from the spacer rings (E and F) and the associated ring plane. [g] The tilt angle τ is the angle between the O···O vector of the inside O,O′ substituted aromatic ring and the mean plane of the four corner methylene carbons atoms of the tetracationic cyclophane.

of the macrocyclic polyether through the cavity of the tetracationic cyclophane occurring, as indicated by the maximum separation between the peaks corresponding to the aromatic protons of the 1,4-dioxybenzene rings occupying the inside and alongside positions ($\Delta\delta$ = 2.75 ppm) (Fig. 7(a)). These aromatic protons did not show any chemical shift by cooling down the solution, but they experience broadening, and at 223 K they appear as two broad peaks as an indication of the slow exchange related to the flipping of the 1,4-dioxybenzene rings within the tetracationic cyclophane cavity (Process III "rocking"). At 203 K this motion is frozen, two different singlets of equal intensity appear at δ 1.86 ppm and δ 5.37 ppm (Fig. 7(c)), corresponding to hydrogen atoms directed towards the xylyl spacer and the outside of the cavity, respectively, corresponding to two of the four non-equivalent protons of the 1,4-dioxybenzene ring (the other two being the hydrogen atoms directed towards the triazolyl spacer and the outside of the cavity). By following the coalescence of this peak at 236 K, the energy associated to the process could be calculated as $\Delta G^{\ddagger}$ = 41.0 kJ mol^{-1} (Table 5), a value slightly lower to the calculated energy of process III for the [2]catenane with one *p*-xylyl spacer and one *m*-xylyl units as spacers of the bipyridinium units in the tetracationic cyclophane (43.93 kJ mol^{-1}).[16]

The tetracationic cyclophane aromatic protons also have signals which exhibit dynamic behaviour. Thus, by cooling the CD_3COCD_3 solution of the [2]catenane **10**·4PF$_6$, the ^{1}H NMR spectrum shows broadening for all the α- and β-CH protons of the bipyridinium unit as well as the *p*-xylyl spacer protons, indicating that circumrotation of the tetracationic cyclophane through the macrocyclic polyether (process II) is slowing down (Fig. 7(b)). At 203 K, the α-CH protons of the bipyridinium unit closer to the xylyl spacer (α-CH(B)) appear as two sets of signals at δ 9.34 and 9.11 ppm, and the α-CH protons of the bipyridinium unit closer to the triazole spacer (α-CH(T)) appear as two sets of signals at δ 9.46 and 9.37 ppm (Fig. 7(c)), with no exchange of the positions. The coalescence of α-CH(B) at 258 K allowed the energy associated to the process to be calculated as $\Delta G^{\ddagger}$ = 50.63 kJ mol^{-1} (Table 5). The same energy value was obtained for this process II (Table 5), when calculated from the coalescence of the methylene protons linked to the xylyl spacer (CH_2N^+(B)).

The ^{1}H NMR spectrum of the [2]catenane **11**·4PF$_6$ in CD_3CN solution at room temperature also shows that circumrotation of the macrocyclic polyether through the cavity of the tetracationic cyclophane is not occurring in this case, with no exchange of the 1,4-dioxybenzene rings between the inside and alongside positions on the NMR timescale. This statement is based on the chemical shift values for the only *one* signal corresponding to the 1,4-dioxybenzene ring alongside the tetracation cavity (δ 6.23 ppm) and the only *one* signal corresponding to the 1,4-dioxybenzene ring inside the tetracation cavity (δ 3.65 ppm), with a maximum separation of $\Delta\delta$ = 2.58 ppm (Fig. 8(a), Table 4), a higher separation compared with the maximum separation for the [2]catenane incorporating two *m*-xylyl units as spacers of the bipyridinium units in the tetracationic cyclophane,[16] possibly because of the close contact in between the nitrogen atom of the triazole spacer and the protons of the included dioxybenzene unit seen in the crystal structure of this compound. Warming the CD_3CN solution to 343 K (Fig. 8(b)) showed broadening for the aromatic hydrogen of the 1,4-dioxybenzene rings, indicating a slow exchange but the energy associated with this process (process I) could not be calculated.

The ^{1}H NMR spectrum of **11**·4PF$_6$, recorded in CD_3COCD_3 solution is very similar to that recorded in CD_3CN solution at room temperature. The singlets for the aromatic protons of the 1,4-dioxybenzene rings occupying the

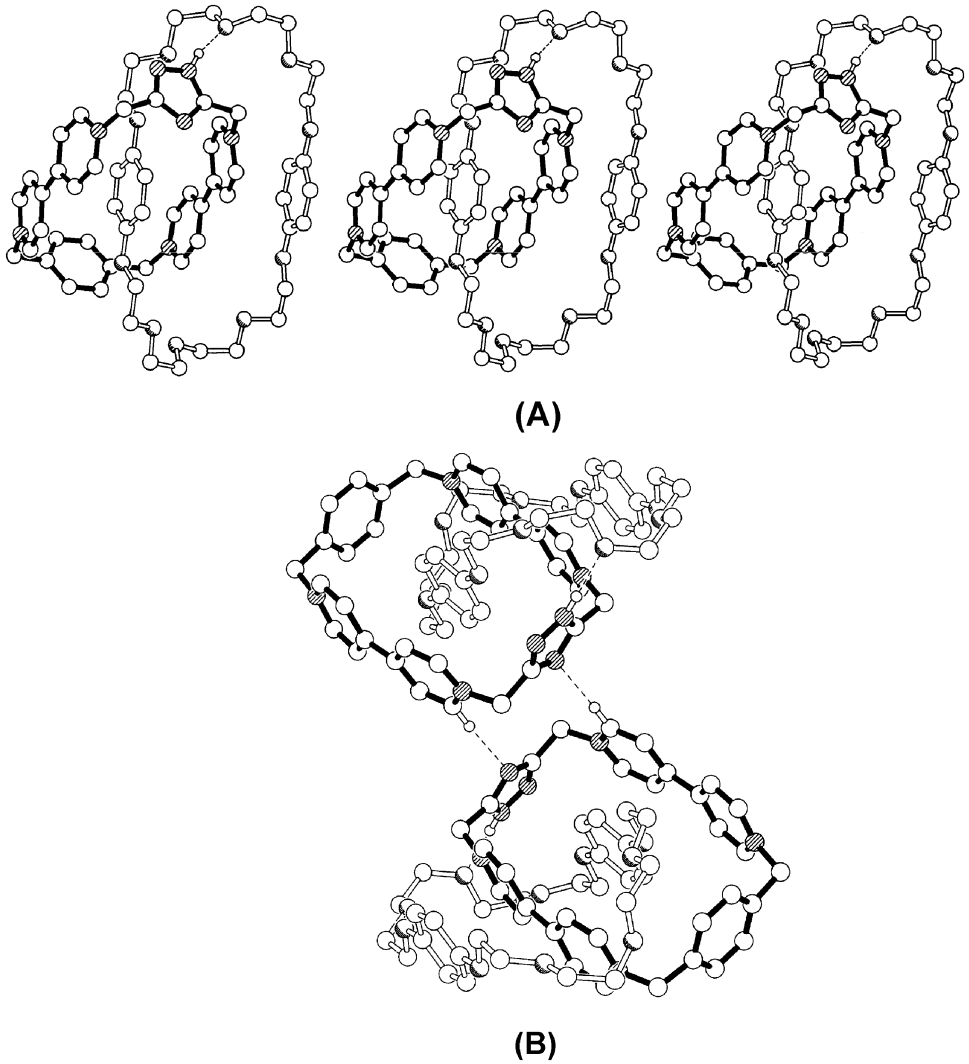

Fig. 2 (A) Part of one of the polar stacks of [2]catenanes present in the crystals of **10**·4PF_6. (B) The C–H···N linking of the [2]catenanes of adjacent polar stacks in the structure of **10**·4PF_6. The hydrogen bonding geometry, C···N, H···N (Å), C–H···N (°), is 3.40, 2.45, 172.

inside and alongside positions at δ 6.31 and δ 3.71 ppm, respectively ($\Delta\delta$ = 2.60 ppm) (Fig. 9(a)) indicates that Process I is frozen, with no changes in their chemical shifts after cooling down the solution. The ''inside'' 1,4-dioxybenzene aromatic protons experience broadening (Fig. 9(b)), and at 198 K (Fig. 9(c)) two different peaks of equal intensity appear at δ 2.84 ppm and δ 4.68 ppm ($\Delta\delta$ = 1.84 ppm), since ''rocking'' does not take place. By following the coalescence of these peaks at 255 K, the energy associated to the process could be calculated as $\Delta G^{\ddagger}$ = 46.02 kJ mol^{-1} (Table 5).

The ^{1}H NMR spectra for the tetracationic cyclophane within the [2]catenane **11**·4PF_6, are also temperature dependent. In CD_3COCD_3 solution at room temperature, broad signals at δ 8.81, 7.82 and 5.92 ppm corresponding to the α-CH, β-CH protons of the bipyridinium unit, and the CH_2 group linked to the 1,2,4-triazole ring (Fig. 9(a)), which indicates that process II is already slow on the NMR timescale. Cooling down the solution induces broadening for all these peaks, and the α- and β-CH protons appear as four peaks each at 198 K, once process II is frozen (Fig. 9(c)). The coalescence of the α- and β-CH protons at 265 and 271, respectively allowed the calculation of the energy barrier associated to the process $\Delta G^{\ddagger}$ = 53.14 kJ mol^{-1} and $\Delta G^{\ddagger}$ = 50.21 kJ mol^{-1} (Table 5).

In this case, the prototropic tautomerism could also be evaluated ($\Delta G^{\ddagger}$ = 54.39 kJ mol^{-1}) (Table 5) by following the coalescence of the methylene hydrogen atoms linked to the 1,2,4-triazole unit, which evolves from a broad singlet at room temperature δ 6.30 ppm (Fig. 9(a)), to a broader signal at 271 K (Fig. 9(b)), to two signals (δ 6.04 and 6.51) at 198 K (Fig. 9(c)). The energy associated to this process is considerably higher comparing to the free tetracationic component (Table 5), as a consequence of the intramolecular (intercomponent) hydrogen bond within the [2]catenane molecular structure.

NMR spectroscopy allows identifying and quantifying the various dynamic processes operating within these systems, including prototropic tautomerism of the triazole rings, potentially usable as elements of control of switchability.

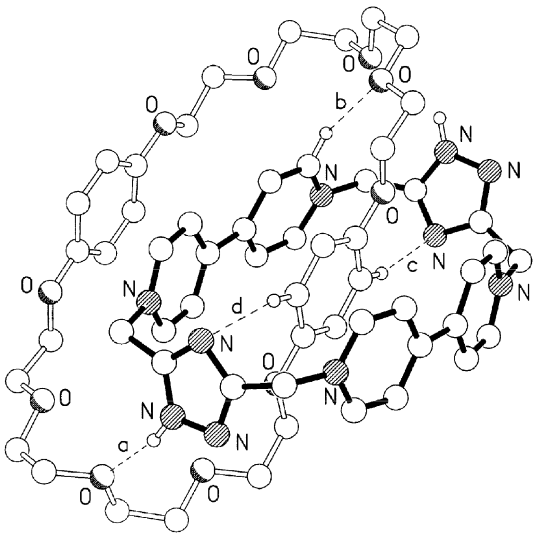

Fig. 3 The molecular structure of **11**·4PF_6 showing the intra[2]catenane hydrogen bonding interactions. The hydrogen bonding geometries are (a) N···O, H···O (Å), N–H···O (°), 2.79, 1.90, 167; (b) C···O, H···O (Å), C–H···O (°), 3.28, 2.44, 146; (c) C···N, H···N (Å), C–H···N (°), 3.38, 2.45, 164; (d) C···N, H···N (Å), C–H···N (°), 3.55, 2.61, 165.

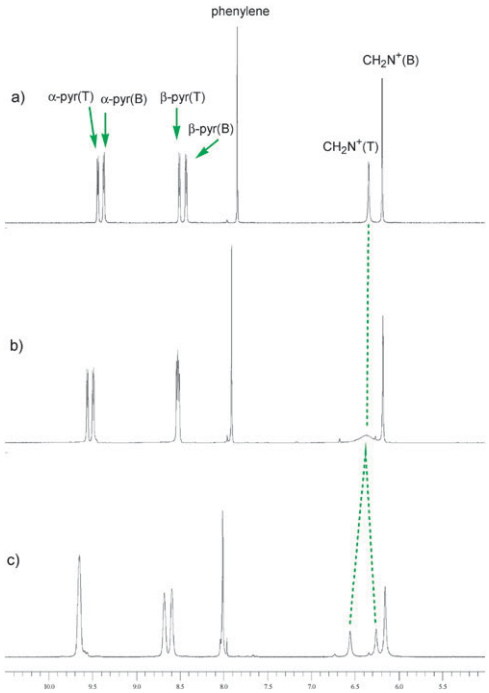

Fig. 4 ^{1}H NMR spectra for cyclophane **6**·4PF_6 in CD_3COCD_3 at (a) 298 K, (b) 233 K, (c) 198 K.

Complexation studies, chemical stability in basic media and switchability

Initially, complexation was studied by UV-Vis technique in acetonitrile solution. An equimolecular mixture of the tetracationic cyclophane **6**·4PF_6 and the extended open chain polyether **5** in acetonitrile showed an intense charge transfer band at λ = 472 nm, indicating π–π interactions between the two components, and therefore the formation of the complex, for which the stability constant (K_a = 1334 M^{-1}) was obtained

Table 4 ^{1}H NMR data for the tetracationic cyclophanes **6**·4PF_6, **7**·4PF_6 and the [2]catenanes **10**·4PF_6 and **11**·4PF_6[a]

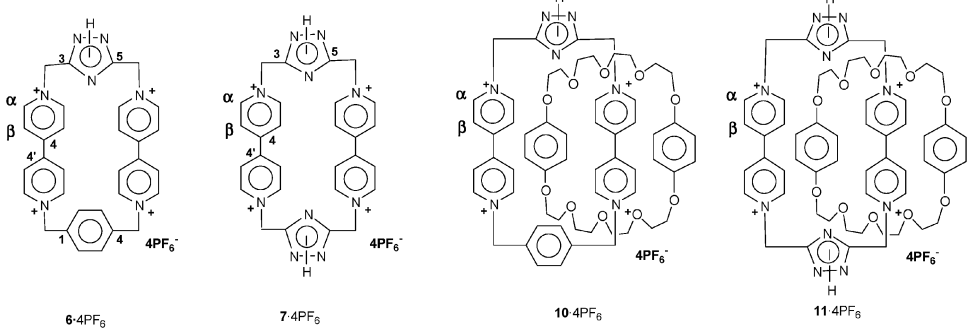

6·4PF_6 **7**·4PF_6 **10**·4PF_6 **11**·4PF_6

		Tetracationic component							Macrocyclic polyether		
	NH	αCH(T)	αCH(B)	βCH(T)	βCH(B)	C_6H_4	CH_2N^+(T)	CH_2N^+(B)	OC_6H_4O		OCH_2
6·4PF_6[b]	[c]	8.95	8.88	8.11	8.11	7.63	5.89	5.78	—		—
7·4PF_6[b]	[c]	8.89	—	8.13	—	—	5.92	—	—		—
8[b]	—	—	—	—	—	—	—	—	6.76		3.60–3.95
10·4PF_6[b]	4.59	8.90 (−0.05)	8.86 (+0.02)	7.78 (−0.33)	7.71 (−0.40)	7.80 (+0.17)	5.96 (+0.07)	5.70 (−0.08)	(a) 6.21 (−0.55)	(i) 3.95 (−2.81)	3.96–3.37
10·4PF_6[d]	4.97[c]	9.35	9.19	8.35	8.24	8.05	6.27	6.05	(a) 6.27	(i) 4.02	3.46–4.06
11·4PF_6[b]	4.72	8.81 (−0.08)	—	7.82 (−0.31)	—	—	5.92 (0.00)	—	(a) 6.23 (−0.53)	(i) 3.65 (−3.11)	4.01–3.36
11·4PF_6[d]	5.02[c]	9.22	—	8.39	—	—	6.31	—	(a) 6.31	(i) 3.71	3.45–4.04

[a] Numbers in parenthesis refer to the variation in chemical shift (Δδ) between the free component and the [2]catenane. Compound **8** is included for comparison. The letters (i) and (a) indicate the inside and alongside benzene rings, respectively, within the catenane. [b] CD_3CN (300 MHz). [c] Broad signal. [d] CD_3COCD_3 (500 MHz).

Table 5 Kinetic and thermodynamic parameters calculated from ^{1}H NMR spectra in CD_3COCD_3 at variable temperature for the tetracationic cyclophanes **6**·4PF_6, **7**·4PF_6 and the [2]catenanes **10**·4PF_6 and **11**·4PF_6

Compound	Protons observed	$\Delta\nu$/Hz	K_c/s^{-1}	T_c/K	$\Delta G_c^{\ddagger}$/kJ mol	Process
6·4PF_6	OCH_2-Tr	149.5	333	233	45.19	Tautom. NH
7·4PF_6	OCH_2-Tr	150.0	333	224	43.51	Tautom. NH
10·4PF_6	α-CH Bipy	122	271	258	50.63	II
	CH_2N^+	72.5	161	253	50.63	II
	OC_6H_4O	1753	3894	236	41.0	III
11·4PF_6	α-CH Bipy	203	451	265	53.14	II
	β-CH Bipy	139	309	271	50.21	II
	OC_6H_4O	920	2048	255	46.02	III
	OCH_2-Tr	234	520	283	54.39	Tautom. NH

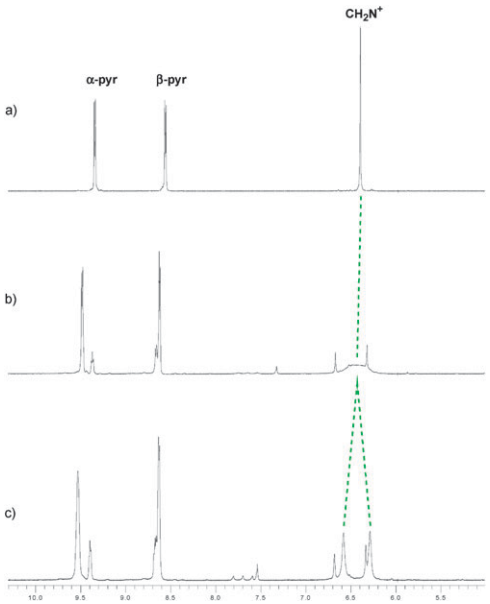

Fig. 5 ^{1}H NMR spectra for cyclophane **7**·4PF_6 in CD_3COCD_3 at (a) 298 K, (b) 224 K, (c) 198 K.

by titration, and the complexation energy calculated ($-\Delta G^{\circ}$ = 17.57 kJ mol^{-1}). In the same conditions, an equimolar mixture of cyclobis(paraquat-*p*-phenylene) **19**·4PF_6 and **5** forms a stronger complex[11] (Chart 6). Although there is no a straightforward link between energy of complexation and binding constants, the weaker binding between **6**·4PF_6 and **5** indicates the poorer recognition between π-rich moieties and π-deficient units containing triazole rings, as a consequence of lacking some of the non covalent interactions driving to their formation.**

When **13**·PF_6 was treated with 1 equivalent of hindered bases such as DBU, both in CD_3CN and DMSO-d_6 solutions, the corresponding betaine **16** was formed (Chart 7), as indicated by the upfield shift of the azolate hydrogen atoms by ^{1}H NMR studies (Table 6). For instance, in DMSO-d_6 the most affected hydrogen atom is H-3(5) on the triazolate ring, which appears at δ 7.62 ppm for the betaine **16**, whereas for the salt **13**·PF_6 it appears at δ 8.65 ppm ($\Delta\delta$ = −1.03 ppm), as well as the methylene protons, which move upfield at δ 5.81 ($\Delta\delta$ = −0.23 ppm) (Table 6). These values agree with chemical shifts for compound

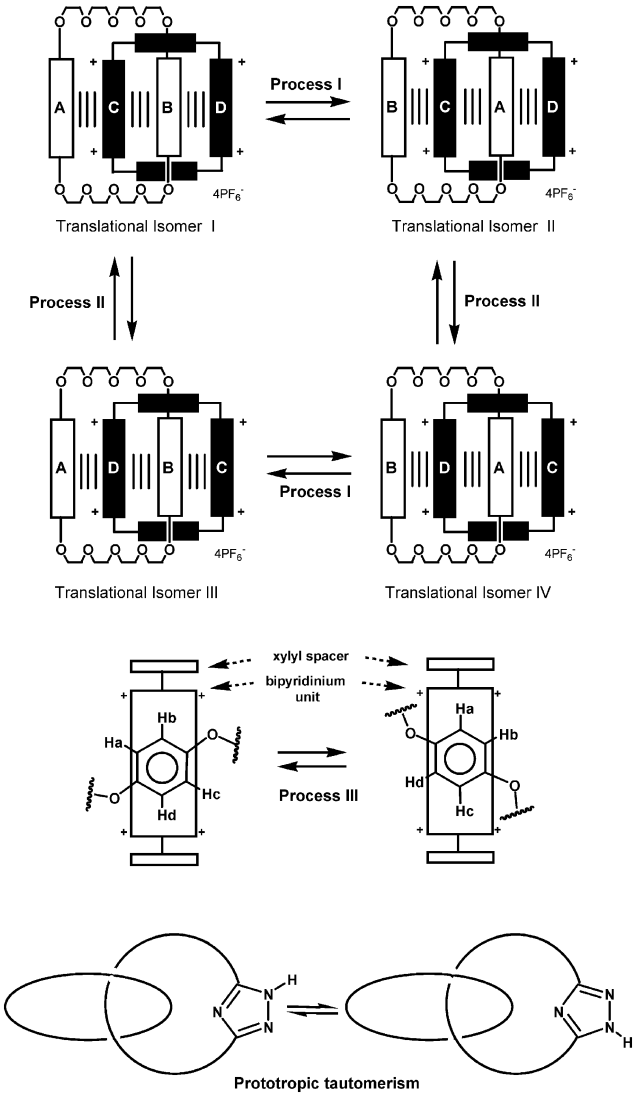

Chart 5 Dynamic processes operating in the described [2]catenanes. Process I refers to the circumrotation of the macrocyclic polyether through the cavity of the tetracationic cyclophane. Process II relates to the circumrotation of the tetracationic cyclophane through the macrocyclic polyether. The number of isomers depends on the symmetry of the macrocyclic components. Process III "rocking" refers to the flipping of the 1,4-dioxybenzene rings within the tetracationic cyclophane cavity. The triazole ring experiences prototropic tautomerism.

** The X-ray crystal study of the catenane **10**·4PF_6 shows the loss of one T-type interaction compared to previously described [2]catenanes.

16 prepared by treatment with an anionic exchange resin (see Chart 4), and chemical shift values for previously described

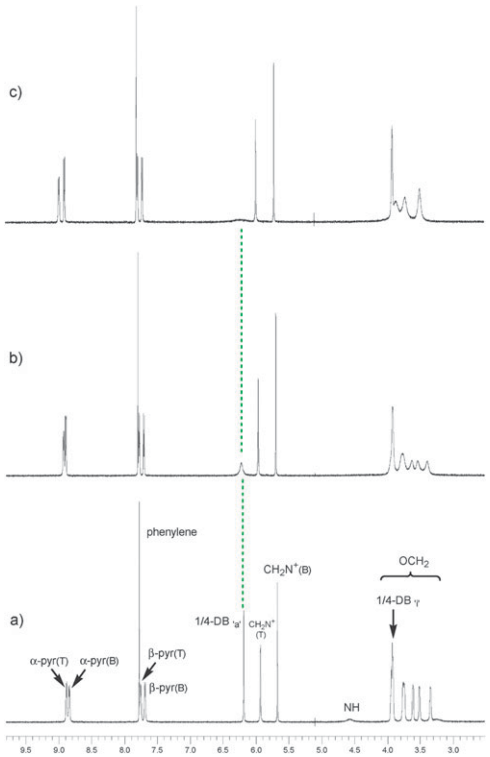

Fig. 6 ^{1}H NMR spectra for [2]catenane **10**·4PF_6 in CD_3CN at (a) 298 K, (b) 323 K, (c) 343 K.

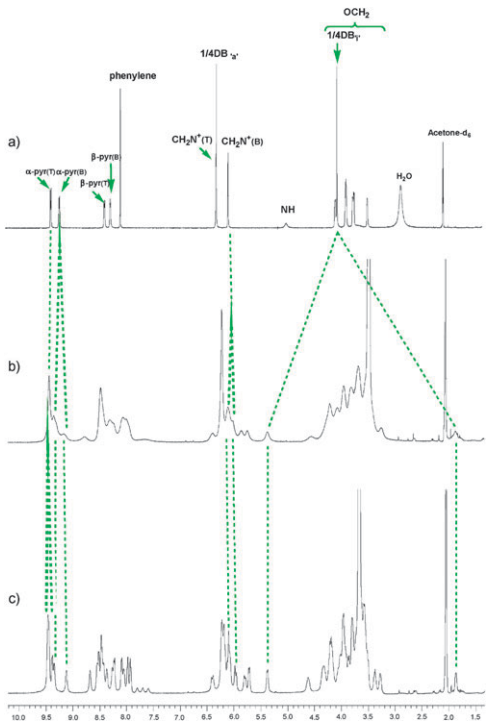

Fig. 7 ^{1}H NMR spectra for [2]catenane **10**·4PF_6 in CD_3COCD_3 at (a) 298 K, (b) 223 K, (c) 203 K.

triazolatemethylenepyridinium compounds.[14] Along with **16**, decomposition products were formed, which ratio increased by the addition of an excess of DBU with respect to **13**·PF_6.

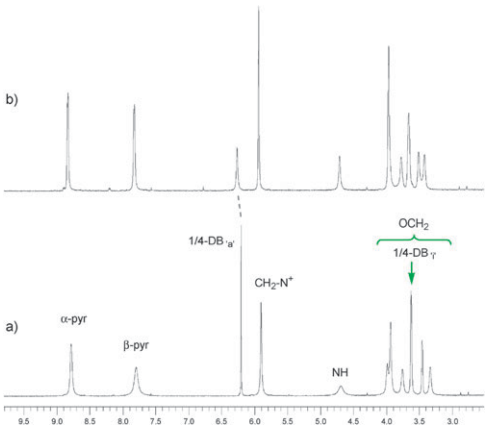

Fig. 8 ^{1}H NMR spectra for [2]catenane **11**·4PF_6 in CD_3CN at (a) 298 K, (b) 343 K.

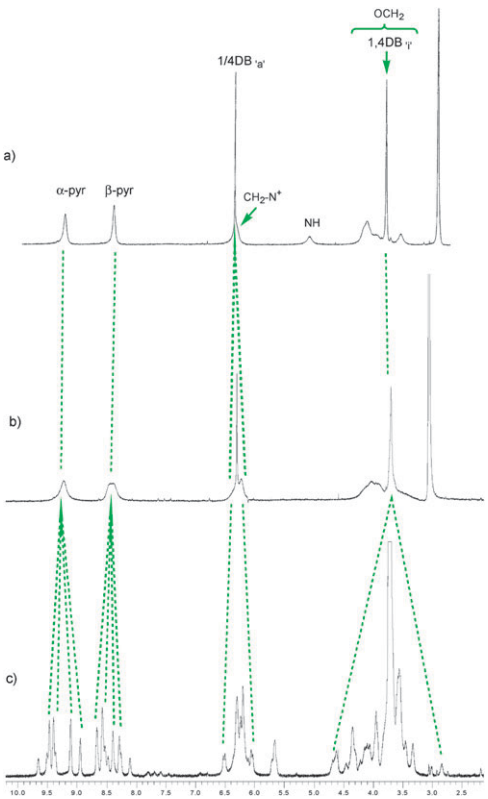

Fig. 9 ^{1}H NMR spectra for [2]catenane **11**·4PF_6 in CD_3COCD_3 at (a) 298 K, (b) 271 K, (c) 198 K.

On the other hand, the equimolar mixture of **13**·PF_6 and the macrocyclic polyether **8** in CD_3CN did not show any color change characteristic of a charge transfer band, indicating the lack of π–π interactions between the two components, and therefore the complex does not form at all. Also, the equimolar mixture of the same components in CD_3CN at 25 °C did not indicated the formation of a complex, with no significant changes in the chemical shifts of the components, as shown by ^{1}H NMR (Table 6). Addition of DBU to the mixture only showed the formation of decomposition products (Chart 7). However, addition of 5 equivalents of trifluoroacetic acid

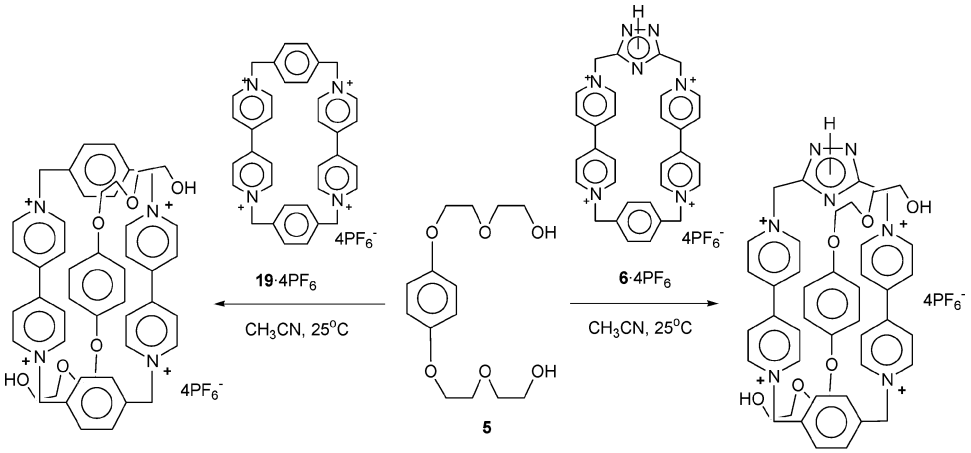

1:1 Complex of **5** with	K_a (M^{-1})	$-\Delta G^o$ ($kJ \cdot mol^{-1}$)
6·4PF_6	1334	17.57
19·4PF_6	2220	19.25

Chart 6 Stability constant values (K_a) and complexation energy ($-\Delta G^o$) for he complexes of **5** with the cyclophanes **6**·4PF_6 (spectrophotometric determination at λ_{max} = 472 nm) and **19**·4PF_6 (spectrophotometric determination at λ_{max} = 467 nm).[11]

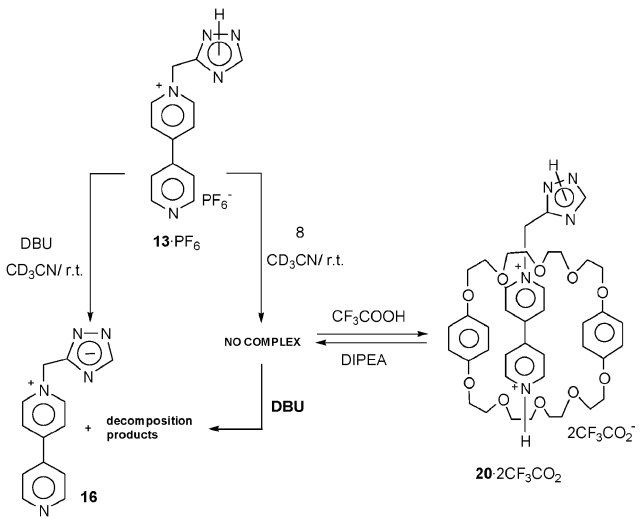

Chart 7

induced the formation of an intense orange color, indicating—after protonation of **13**·PF_6—the formation of the complex **20**·2CF_3CO_2 (Chart 7). The ^{1}H NMR spectrum shows upfield shifts for the β-CH bipyridinium hydrogen atoms ($\Delta\delta$ = −0.31 ppm), the 1,4-dioxybenzene unit ($\Delta\delta$ = −0.25 ppm), and the α-CH_2 of the polyether chain ($\Delta\delta$ = −0.26 ppm), as well as the downfield shift of the methylene for the dication ($\Delta\delta$ = +0.23 ppm), characteristic of the complex **20**·2CF_3CO_2, and the inclusion of the bipyridinium unit within the 1,4-dioxybenzene units (Table 6). Subsequent addition of a base as DIPEA induces deprotonation followed by decomplexation, restoring the initial situation with no observation of decomposition products, and the chemical switch shows reversibility (Chart 7).

Addition of 2 equivalents of DBU to the salt **14**·2PF_6 both in CD_3CN and DMSO-d_6 solutions resulted in the formation of a blue precipitate, and broadening of the ^{1}H NMR signals, as a consequence of the instability of the bipyridinium salts in the presence of triazolate anions (Chart 8).[10] The equimolar mixture of **14**·2PF_6 and the macrocyclic polyether **8** in CD_3CN induced the formation of a red solution, indicating the formation of the complex **21**·2PF_6 (Chart 8). The complex is characterized by the ^{1}H NMR spectrum, which shows upfield shifts for the β-CH bipyridinium hydrogen atoms ($\Delta\delta$ = −0.23 ppm), the 1,4-dioxybenzene unit ($\Delta\delta$ = −0.26 ppm), and the α-CH_2 of the polyether chain ($\Delta\delta$ = −0.21 ppm) (Table 6). Addition of 2 equivalents of DBU to this solution of **21**·2PF_6 induced decomplexation and, furthermore, decomposition of the bipyridinium moiety (Chart 8).

For the salt **15**·4PF_6, addition of 1 equivalent of DBU to both CD_3CN and DMSO-d_6 solutions resulted in the formation of a blue precipitate, and broadening of the ^{1}H NMR signals (Chart 9). The equimolar mixture of **15**·4PF_6 and the macrocyclic polyether **8** in CD_3CN induced the formation of a red solution, indicating the formation of the complex **22**·4PF_6 (Chart 9). The complex is characterized by the ^{1}H NMR spectrum, which shows the most affected protons are those of the 1,4-dioxybenzene unit ($\Delta\delta$ = −0.53 ppm) (Table 6). There is also an upfield shift for the β-CH bipyridinium hydrogen atoms ($\Delta\delta$ = −0.27 ppm), and the α-CH_2 of the polyether chain ($\Delta\delta$ = −0.21 ppm). Addition of another equivalent of the macrocyclic polyether **8** induced a further upfield shift of the β-CH bipyridinium hydrogen atoms ($\Delta\delta$ = −0.34 ppm) (Table 6), indicating a stronger π–π interaction between the components.

Again, addition of 1 equivalent of DBU to this solution of **22**·4PF_6 induced decomplexation and, furthermore, decomposition of the bipyridinium moiety (Chart 9).

Different complexes of the macrocyclic polyether **8** and triazole containing pyridyl-pyridinium **13**·PF_6 as well as bipyridinium systems **14**·2PF_6 and **15**·4PF_6 have been formed, proving difficult to make chemically compatible the bipyridinium unit in the presence of triazolate anions, which may

Table 6 ^{1}H NMR data for the tetracationic salts **13**·PF_6, **14**·$2PF_6$, **15**·$4PF_6$, the betaine **16**, the complexes **21**·$2PF_6$, **22**·$4PF_6$, and acid–base molecular switch **20**·$2CF_3CO_2$

Compound	Hα-pyr$^+$	Hα-pyr	Hβ-pyr$^+$	Hβ-pyr	H-3(5)	CH_2-T	CH_2-B	C_6H_5	C_6H_4	OCH_2-α
13·PF_6[a]	9.30	8.87	8.65	8.02	8.65	6.04	—	—	—	—
16[a]	9.25	8.84	8.57	7.98	7.69	5.85	—	—	—	—
$\Delta\delta$[b]	−0.05	−0.03	−0.08	−0.04	−0.96	−0.19	—	—	—	—
13·PF_6 + DBU[a]	9.23	8.84	8.56	7.86	7.62	5.81	—	—	—	—
$\Delta\delta$	−0.07	−0.03	−0.09	−0.04	−1.03	−0.23	—	—	—	—
13·PF_6[c]	8.94	8.85	8.35	7.80	8.37	5.87	—	—	—	—
13·PF_6 + DBU[c]	8.96	8.83	8.28	7.77	7.86	5.78	—	—	—	—
$\Delta\delta$	+0.02	−0.02	−0.07	−0.03	−0.51	−0.09	—	—	—	—
13·PF_6 + **8**[c]	8.92	8.84	8.32	7.77	8.38	5.86			6.73	3.97
$\Delta\delta$	−0.02	−0.01	−0.03	−0.03	+0.01	−0.01			−0.03	−0.01
20·$2CF_3CO_2$[c]	9.06	8.84	8.01	7.94	8.46	6.09			6.48	3.71
$\Delta\delta$	+0.14	0.00	−0.31	+0.17	+0.08	+0.23			−0.25	−0.26
20·$2CF_3CO_2$ + DIPEA[c]	9.00	8.83	8.32	7.77	8.32	5.92			6.73	3.96
14·$2PF_6$[c]	9.08	—	8.42	—	8.39	5.94	—	—	—	—
21·$2PF_6$[c]	9.07	—	8.19	—	8.41	5.99	—	—	6.50	3.77
$\Delta\delta$	−0.01	—	−0.23	—	+0.02	+0.05	—	—	−0.26	−0.21
15·$4PF_6$	9.02/8.98	—	8.42/8.38	—	—	5.93	5.83	7.52	—	—
22·$4PF_6$[c] (1 : 1)[d]	8.97	—	8.17	—		6.00	5.83	7.53	6.23	3.71
$\Delta\delta$	−0.03	—	−0.23	—		+0.07	0.00	+0.01	−0.53	−0.27
22·$4PF_6$[c] (1 : 2)[d]	8.97	—	8.06	—		6.04	5.84	7.54	6.34	3.70
$\Delta\delta$	−0.03	—	−0.34	—		+0.11	+0.01	+0.02	−0.42	−0.28
8[c]	—	—	—	—	—	—	—	—	6.76	3.98

[a] In DMSO-d_6. [b] $\Delta\delta$ corresponds to variation in chemical shift between the betaine and the salt. [c] In CD_3CN. [d] Equivalents of **8** added to **15**·$4PF_6$.

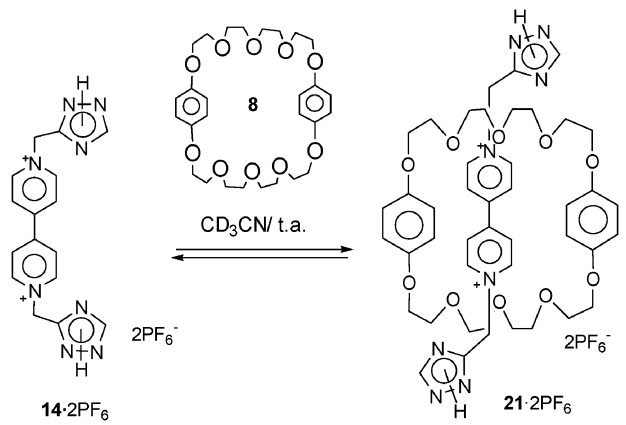

Chart 8

preclude using the prototropic tautomerism as the control key of switches built up with these components.

Conclusions

It is possible to construct tetracationic cyclophanes as well as [2]catenanes incorporating 1*H*-1,2,4-triazole units as spacers of the π-deficient component. These heteroaromatic moieties influence especially (a) the solid-state structure of the [2]catenanes, since **10**·$4PF_6$ forms enantiomeric pairs as a consequence of the establishment of intermolecular hydrogen bonds where the triazole ring is involved, and **11**·$4PF_6$, very unusually, does not form polar stacks at all, and (b) the dynamic behaviour in solution for the introduction of tautomeric prototropism

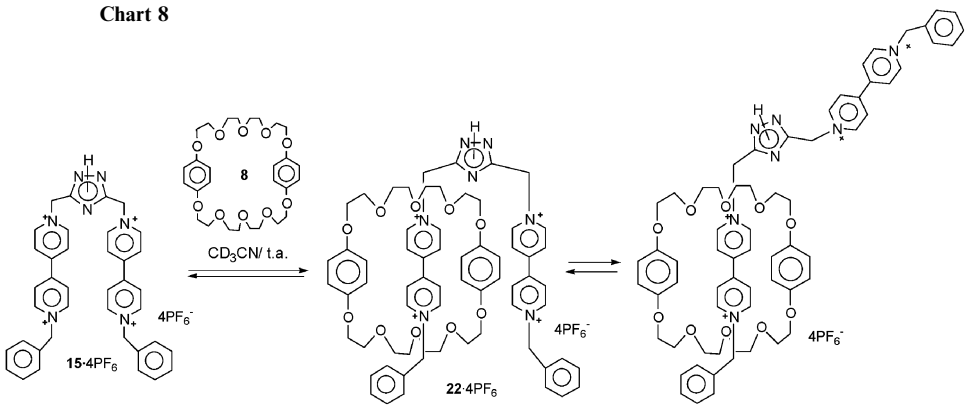

Chart 9

process. Furthermore, a model of a chemical switch based on protonation of the pyridyl-pyridinium compound **13**·PF_6 to the bipyridinium complex **20**·$2CF_3CO_2$ has been described. However, the instability of bipyridinium units in basic media, including triazolate anions, makes its use as an element of switching within the systems a significant challenge.

Experimental

General methods

Melting points: CTP–MP 300 hot-plate apparatus with ASTM 2C thermometer. IR (KBr disks): Nicolet 205 FT spectrophotometer. ^{1}H NMR: Varian Gemini 200, Varian Gemini 350 and Varian VXR 500 spectrometers (200 MHz, and 350 and 500 MHz). ^{13}C NMR: Varian Gemini 200 and Varian Gemini 300 spectrometer (50.3 and 75.4 MHz). HMQC and HMBC: Varian VXR 500 spectrometer (500 MHz). COSY-2D and ROESY-2D: Bruker 500 spectrometer (500 MHz). NMR spectra were determined in $CDCl_3$, $(CD_3)_2SO$, CD_3CN, CD_3OD or $(CD_3)_2CO$, and chemical shifts are expressed in parts per million (δ) relative to the central peak of the solvent. ES-MS and FAB-MS: VG-Quattro mass spectrometer. TLC was performed on Merck precoated 60 F_{254} silica gel plates in the solvent system methanol–aqueous 2 M ammonium chloride–nitromethane (6 : 3 : 1) as developing solvent; and the spots were located with UV light and developed with a 10% aqueous solution of potassium iodide or 3% aqueous solution of hexachloroplatinic acid. Chromatography: SDS silica oxide 60 ACC (30–75 μm) and Merck aluminum oxide 90 standardized. UV-Vis: CARY-Varian spectrophotometer. When a rotary evaporator was used, the bath temperature was 25 °C. In general, the compounds were dried overnight at 25 °C in a vacuum oven. Microanalyses were performed on a Carlo Erba Fisons EA1108 analyzer in the *Serveis Científico-Tècnics* (*UB*). HR-MS: Autospec/VG analyzer, recorded in *the Departament de Química Orgànica Biològica* (*C.S.I.C.*) *de Barcelona*. Experiments at high pressure were performed using an ANDREAS HOFER press of 14 kbar; reactions were carried out in a thermally sealed Teflon tube located in the press cylinder, and using *n*-hexane as the external solvent. Solvents were distilled under nitrogen or argon over a variety of drying agents.[17] DMF and DME were distilled over calcium hydride and stored with molecular sieve (4 Å). CH_3CN was HPLC grade (SDS) and dried with molecular sieve (4 Å). When an anionic exchange resin was used, the previously established protocol was employed.[8]

Materials

Commercial compounds: Ammonium hexafluorophosphate, 4,4′-bipyridine, 1,4-bis(bromomethyl)benzene **4**, 1,4-bis(chloromethyl)benzene **9**, 1,8-diazabicyclo[5.4.0]undec-7-ene (DBU), diisopropylethylamine (DIPEA), NaH 95% dry were purchased from Aldrich. Compounds prepared according to literature procedures: 1,1-[1,4-phenylenebis(methylene)]-bis-4,4′-pyridylpyridinium **1**·$2PF_6$,[11] 3,5-bis(chloromethyl)-1*H*-1,2,4-triazole **3**,[8] 1,4-bis[2-(2-hydroxyethoxy)ethoxy]benzene **5**,[11] bis-*p*-phenylene-34-crown-10 (BPP34C10) **8**,[11] 3(5)-chloromethyl-1*H*-1,2,4-triazole **12**,[14] cyclobis(paraquat-*p*-phenylene) **19**·$4PF_6$.[11]

Syntheses

1,1′-[3,5-1*H*-1,2,4-Triazolylbis(methylene)]bis-4,4′-pyridylpyridinium bis(hexafluorophosphate) 2·2PF$_6$. A solution of 3,5-bis(chloromethyl)-1*H*-1,2,4-triazole **3** (0.55 g, 3.31 mmol) in anhydrous DMF (60 mL) was added over 5 h at 80 °C to a solution of 4,4′-bipyridine (1.14 g, 7.28 mmol) in anhydrous DMF (40 mL). During the addition a pale pink color developed and after 15 h under vigorous stirring at 80 °C, the suspension obtained was filtered, and the solvent was removed *in vacuo*. The residue was washed in anhydrous ether (3 × 20 mL). The solid precipitated was washed in anhydrous acetone (3 × 20 mL) and filtered. The residue was purified by column chromatography [SiO_2, MeOH–2 M NH_4Cl–CH_3NO_2 6 : 3 : 1]. The fractions containing the product were combined and concentrated, and the residue was dissolved in H_2O (10 mL) before a saturated aqueous NH_4PF_6 solution was added until no further precipitation occurred. The suspension was filtered off, and the solid recrystallized from H_2O–acetone to give **2**·$2PF_6$ as a white solid (0.69 g, 30%); mp 216–218 °C (decomp.); ^{1}H NMR (200 MHz, CD_3CN, 25 °C): δ 8.88 (d, J = 7.0 Hz, 4H, α-pyr$^+$); 8.84 (d, J = 6.0 Hz, 4H, α-pyr); 8.35 (d, J = 7.4 Hz, 4H, β-pyr$^+$); 7.78 (d, J = 6.2 Hz, 4H, β-pyr); 5.88 (s, 4H, CH_2); ^{13}C NMR (50.3 MHz, CD_3CN) δ 155.8 (C_q-3.5); 151.8; 146.4; 141.7; 126.7; 122.6; 56.8. Found: C, 40.3; H, 2.4; N, 13.8. Calc. for $C_{24}H_{21}N_7F_{12}P_2$: C, 40.3; H, 2.9; N, 13.7%.

2,11,22,31-Tetraazonia[1.0.1.1.0]paracyclo[1](3,5)triazolophane tetrakis(hexafluorophosphate) 6·4PF$_6$. 1,4-Bis(bromomethyl)-benzene **4** (208 mg, 0.126 mmol), **2**·$2PF_6$ (500 mg, 0.72 mmol) and **5** (513 mg, 1.79 mmol) were dissolved in dry DMF (4 mL) in a high-pressure vessel which was pressurized to 13 kbar for 3 days at room temperature. The red suspension obtained was poured into Et_2O (60 mL), the precipitate was filtered off, washed with Et_2O (2 × 5 mL), and dried. The residue was purified by column chromatography [SiO_2, MeOH–2 M NH_4Cl–CH_3NO_2 5 : 3 : 2]. The fractions containing the product were combined and concentrated, and the residue was dissolved in H_2O (5 mL) before a saturated aqueous NH_4PF_6 solution was added until no further precipitation occurred. The suspension was filtered off, and the solid recrystallized from H_2O–acetone to give **6**·$4PF_6$ as a white solid (118 mg, 15%); mp >300 °C (decomp.); ^{1}H NMR (500 MHz, CD_3COCD_3, 25 °C): δ 9.40 (d, J = 6.5 Hz, 4H, α-CH(T)), 9.34 (d, J = 7.0 Hz, 4H, α-CH(B)), 8.50 (d, J = 7.0 Hz, 4H, β-CH(T)), 7.42 (d, J = 7.0 Hz, 4H, β-CH(B)), 7.83 (s, 4H, C_6H_4)), 6.33 (s, 4H, CH_2N^+(T)), 6.19 (s, 4H, CH_2N^+(B)); ^{1}H NMR (200 MHz, CD_3CN, 25 °C): δ 8.95 (d, J = 6.6 Hz, 4H, α-CH(T)), 8.88 (d, J = 6.8 Hz, 4H, α-CH(B)), 8.11 (d, J = 6.0 Hz, 8H, β-CH), 7.63 (s, 4H, C_6H_4), 5.89 (s, 4H, CH_2N^+(T)), 5.78 (s, 4H, CH_2N^+(B)); ^{13}C NMR (50.3 MHz, CD_3CN): δ 151.1 (C_q-3,5(T)), 150.7 (C_q-4,4′), 147.0 (α-pyr(B)), 145.6 (α-pyr(T)), 137.4 (C_q-1,4(B)), 131.1 (C-2,3,5,6(B)), 128.4 (β-pyr(B)), 127.6 (β-pyr(B)), 65.8

(CH_2(B)), 57.1 (CH_2(T)). Found: C, 35.2; H, 2.9; N, 8.9. Calc. for $C_{32}H_{29}N_7F_{24}P_4$: C, 35.2; H, 2.7; N, 8.9%.

2,11,21,30-Tetraazonia[1.0]paracyclo[1](3,5)triazolophane[1.0]-paracyclo[1](3,5)triazolophane tetrakis(hexafluorophosphate) 7·4PF$_6$. 3,5-Bis(chloromethyl)-1*H*-1,2,4-triazole **3** (171 mg, 1.03 mmol), **2**·2PF$_6$ (600 mg, 0.86 mmol) and **5** (615 mg, 2.15 mmol) were dissolved in dry DMF (4 mL) in a high-pressure vessel which was pressurized to 13 kbar for 3 days at room temperature. The red suspension obtained was poured into Et_2O (50 mL), the precipitate was filtered off, washed with Et_2O (2 × 5 mL), and dried. The residue was purified by column chromatography [SiO_2, MeOH–2 M NH_4Cl–CH_3NO_2 6 : 3 : 1]. The fractions containing the product were combined and concentrated, and the residue was dissolved in H_2O (5 mL) before a saturated aqueous NH_4PF_6 solution was added until no further precipitation occurred. The suspension was filtered off to give **7**·4PF$_6$ as a white solid (32 mg, 3.5%); mp >300 °C (decomp.); ^{1}H NMR (500 MHz, CD_3COCD_3, 25 °C): δ 9.35 (d, J = 6.5 Hz, 8H, α-CH), 8.57 (d, J = 6.5 Hz, 8H, β-CH), 6.40 (s, 8H, CH_2N^+); ^{1}H NMR (200 MHz, CD_3CN, 25 °C): δ 8.89 (d, J = 6.4 Hz, 8H, α-CH), 8.13 (d, J = 6.6 Hz, 8H, β-CH), 5.92 (s, 8H, CH_2N^+); ^{13}C NMR (50.3 MHz, CD_3CN): δ 151.3, 150.6, 145.6, 127.6, 57.5. Found: C, 31.1; H, 2.4; N, 13.0. Calc. for $C_{28}H_{26}N_{10}F_{24}P_4$: C, 31.1; H, 2.4; N, 12.9%.

{[2][1,4,7,10,13,20,23,26,29,32-Decaoxa[13.13]paracyclophane]-[2,11,22,31-tetraazonia[1.0.1.1.0]paracyclo[1](3,5)triazolophane]-catenane} tetrakis(hexafluorophosphate) 10·4PF$_6$

Route A. ***Method 1***: A solution of 3,5-bis(chloromethyl)-1*H*-1,2,4-triazole **3** (34 mg, 0.205 mmol) and NaI (61 mg, 0.41 mmol) in dry DMF (1 mL) was added to a solution of **8** (250 mg, 0.465 mmol) and **1**·2PF$_6$ (132 mg, 0.186 mmol) in dry DMF (3 mL). After 48 h 0.2 equiv. of 3,5-bis(chloromethyl)-1*H*-1,2,4-triazole **3** were added to the solution. After 15 days a pale red color developed and some red precipitate appeared. The suspension was poured into Et_2O (30 mL), the precipitate was filtered off, washed with Et_2O (2 × 5 mL), and dried. The residue was purified by column chromatography [SiO_2, MeOH–2 M NH_4Cl–CH_3NO_2 5.5 : 3 : 1.5]. The fractions containing the product were combined and concentrated, and the residue was dissolved in H_2O (5 mL) before a saturated aqueous NH_4PF_6 solution was added until no further precipitation occurred. The suspension was filtered off, and the solid recrystallized from MeCN–*i*-Pr_2O to give **10**·4PF$_6$ as a red solid (3 mg, 1%).

Method 2: 3,5-Bis(chloromethyl)-1*H*-1,2,4-triazole **3** (37 mg, 0.222 mmol), **1**·2PF$_6$ (132 mg, 0.186 mmol) and **8** (250 mg, 0.465 mmol) were dissolved in dry DMF (2 mL) in a high-pressure vessel which was pressurized to 10 kbar for 3 days at room temperature. The red suspension obtained was poured into Et_2O (30 mL), the precipitate was filtered off, washed with Et_2O (2 × 5 mL), and dried. The residue was purified by column chromatography [SiO_2, MeOH–2 M NH_4Cl–CH_3NO_2 5.5 : 3 : 1.5]. The fractions containing the product were combined and concentrated, and the residue was dissolved in H_2O (5 mL) before a saturated aqueous NH_4PF_6 solution was added until no further precipitation occurred. The suspension was filtered off, and the solid recrystallized from MeCN–*i*-Pr_2O to give **10**·4PF$_6$ as a red solid (18 mg, 6%).

Route B. 1,4-Bis(chloromethyl)benzene **9** (22 mg, 0.126 mmol), **2**·2PF$_6$ (80 mg, 0.114 mmol) and **8** (153 mg, 0.285 mmol) were dissolved in dry DMF (2 mL) in a high-pressure vessel which was pressurized to 10 kbar for 3 days at room temperature. The red suspension obtained was poured into Et_2O (30 mL), the precipitate was filtered off, washed with Et_2O (2 × 5 mL), and dried. The residue was purified by column chromatography [SiO_2, MeOH–2 M NH_4Cl–CH_3NO_2 5.5 : 3 : 1.5]. The fractions containing the product were combined and concentrated, and the residue was dissolved in H_2O (5 mL) before a saturated aqueous NH_4PF_6 solution was added until no further precipitation occurred. The suspension was filtered off, and the solid recrystallized from MeCN–*i*-Pr_2O to give **10**·4PF$_6$ as a red solid (26 mg, 14%).

Mp >300 °C (decomp.); ^{1}H NMR (500 MHz, CD_3COCD_3, 25 °C): δ 9.35 (d, J = 6.5 Hz, 4H, α-CH(T)), 9.19 (d, J = 6.0 Hz, 4H, α-CH(B)), 8.35 (d, J = 5.5 Hz, 4H, β-CH(T), 8.24 (d, J = 6.0 Hz, 4H, β-CH(B)), 8.05 (s, 8H, C_6H_4), 6.27 (s, 4H, CH_2N^+(T)), 6.27 (s, 4H, 1/4DB$_{a'}$), 6.05 (s, 4H, CH_2N^+(B)), 4.97 (br s, 1H, NH), 4.06–3.46 (m, 32H, OCH_2), 4.02 (s, 4H, 1/4DB$_{i'}$); ^{1}H NMR (500 MHz, CD_3CN, 25 °C): δ 8.90 (d, J = 6.5 Hz, 4H, α-CH(T)), 8.86 (d, J = 6.0 Hz, 4H, α-CH(B)), 7.78 (d, J = 6.5 Hz, 4H, β-CH(T)), 7.71 (d, J = 6.0 Hz, 4H, β-CH(B)), 7.80 (s, 8H, C_6H_4), 6.21 (s, 4H, 1/4DB$_{a'}$), 5.96 (s, 4H, CH_2N^+(T)), 5.70 (s, 4H, CH_2N^+(B)), 4.59 (br s, 1H, NH), 3.96–3.37 (m, 32H, OCH_2), 3.95 (s, 4H, 1/4DB$_{i'}$). Found: C, 43.8; H, 4.3; N, 6.0. Calc. for $C_{60}H_{69}N_7O_{10}F_{24}P_4$·$H_2O$: C, 43.8; H, 4.3; N, 5.9%.

{[2][1,4,7,10,13,20,23,26,29,32-Decaoxa[13.13]paracyclophane][2,11,21,30-tetraazonia[1.0]paracyclo[1](3,5)triazolophane[1,0]paracyclo[1](3,5)triazolophane]catenane} tetrakis(hexafluorophosphate) 11·4PF$_6$. 3,5-Bis(chloromethyl)-1*H*-1,2,4-triazole **3** (89 mg, 0.54 mmol), **2**·2PF$_6$ (313 mg, 0.45 mmol) and **8** (600 mg, 1.12 mmol) were dissolved in dry DMF (6 mL) in a high-pressure vessel which was pressurized to 13 kbar for 3 days at room temperature. The red suspension obtained was poured into Et_2O (60 mL), the precipitate was filtered off, washed with Et_2O (2 × 5 mL), and dried. The residue was purified by column chromatography [SiO_2, MeOH–2 M NH_4Cl–CH_3NO_2 6 : 3 : 1]. The fractions containing the product were combined and concentrated, and the residue was dissolved in H_2O (5 mL) before a saturated aqueous NH_4PF_6 solution was added until no further precipitation occurred. The suspension was filtered off, and the solid recrystallized from MeCN–*i*-Pr_2O to give **11**·4PF$_6$ as a red solid (36 mg, 5%); mp >300 °C (decomp.); ^{1}H NMR (500 MHz, CD_3COCD_3, 25 °C): δ 9.22 (br s, 8H, α-CH), 8.39 (br s, 8H, β-CH), 6.31 (br s, 8H, CH_2N^+), 6.31 (s, 4H, 1/4DB$_{a'}$), 5.02 (br s, 2H, NH), 4.04–3.45 (m, 32H, OCH_2), 3.71 (s, 4H, 1/4DB$_{i'}$); ^{1}H NMR (500 MHz, CD_3CN, 25 °C): δ 8.81 (br s, 8H, α-CH), 7.82 (br s, 8H, β-CH), 5.92 (br s, 8H, CH_2N^+), 6.23 (s, 4H, 1/4DB$_{a'}$), 4.72 (br s, 2H, NH), 4.01–3.36 (m, 32H, OCH_2), 3.65 (s, 4H, 1/4DB$_{i'}$). Found: C, 41.2; H, 4.3; N, 8.4. Calc. for $C_{56}H_{66}N_{10}O_{10}F_{24}P_4$: C, 41.5; H, 4.1; N, 8.6%.

1-(3(5)-1*H*-1,2,4-triazolylmethyl)-4,4′-pyridylpyridinium hexafluorophosphate 13·PF$_6$. A solution of 4,4′-bipyridine (731 mg,

4.68 mmol) in anhydrous DMF (25 mL) was added over 6 h at 100 °C to a solution of 3-chloromethyl-1*H*-1,2,4-triazole **12** (250 mg, 2.13 mmol) in anhydrous DMF (40 mL). The solution was heated at 100 °C for 15 h under vigorous stirring. After this the solvent was removed *in vacuo* and the residue obtained was washed in anhydrous ether (3 × 20 mL). The residue was purified by column chromatography [SiO_2, MeOH–2 M NH_4Cl–CH_3NO_2 7.5 : 2 : 0.5]. The fractions containing the product were combined and concentrated, and the residue was dissolved in H_2O (10 mL) before a saturated aqueous NH_4PF_6 solution was added until no further precipitation occurred. The suspension was filtered off, and the solid recrystallized from H_2O–acetone to give **13**·PF_6 as a white solid (362 mg, 44%); mp 186–188 °C; ^{1}H NMR (200 MHz, CD_3CN, 25 °C): δ 8.94 (d, J = 7.0 Hz, 2H,α-pyr$^+$); 8.85 (d, J = 6.4 Hz, 2H, α-pyr); 8.37 (s, 1H, $H_{3,5}$), 8.35 (d, J = 7.0 Hz, 2H, β-pyr$^+$); 7.80 (d, J = 6.4 Hz, 4H, β-pyr); 5.87 (s, 2H, CH_2); ^{13}C NMR (50.3 MHz, CD_3CN) δ 155.6, 151.7, 146.2, 141.9, 126.8, 122.7, 58.3; ESIMS (60 eV): m/z 238 ([M + 3PF_6]$^+$, 100%).

1,1′-Bis(3(5)-(1*H*-1,2,4-triazolyl)methyl)-4,4′-bipyridinium bis-(hexafluorophosphate) 14·2PF$_6$. A solution of 4,4′-bipyridine (95 mg, 0.61 mmol) and 3-chloromethyl-1*H*-1,2,4-triazole **12** (150 mg, 1,28 mmol) in anhydrous DMF (2 mL) was heated at 100 °C for 15 h under vigorous stirring. The suspension obtained was filtered off, washed with CH_2Cl_2 (2 × 5 mL), and dried. The residue was purified by column chromatography [SiO_2, MeOH/NH_4Cl 2M/CH_3NO_2 6 : 3 : 1]. The fractions containing the product were combined and concentrated, and the residue was dissolved in H_2O (5 mL) before a saturated aqueous NH_4PF_6 solution was added until no further precipitation occurred. The suspension was filtered off, and the solid recrystallized from H_2O–acetone to give **14**·2PF_6 as a white solid (285 mg, 77%); mp 240–241 °C; ^{1}H NMR (200 MHz, CD_3CN, 25 °C): δ 9.08 (d, J = 6.8 Hz, 4H, α-pyr$^+$); 8.39 (s, 2H, $H_{3,5}$), 8.42 (d, J = 7.0 Hz, 4H, β-pyr$^+$); 5.94 (s, 4H, CH_2); ^{13}C NMR (50.3 MHz, CD_3CN) δ 151.3, 149.8, 146.8, 145.9, 128.1, 58.9; ESIMS (60 eV): m/z 465 ([M + 3PF_6]$^+$, 38%), 161 ([M/2]$^{2+}$, 9). Found: C, 30.3; H, 2.6; N, 17.6. Calc. for $C_{16}H_{16}N_8F_{12}P_2$·H_2O: C, 30.6; H, 2.9; N, 17.8%.

3,5-Bis(1-(4,4′-(1′-benzyl)bipyridyl)methyl)-1*H*-1,2,4-triazole tetrakis(hexafluorophosphate) 15·4PF$_6$. A solution of **2**·2PF_6 (400 mg, 0.57 mmol) and benzyl bromide (0.34 mL, 2.87 mmol) in anhydrous DMF (2 mL) was heated at 100 °C for 15 h under vigorous stirring. The suspension obtained was filtered off, washed with Et_2O (2 × 20 mL), and dried. The residue obtained was dissolved in H_2O (5 mL) before a saturated aqueous NH_4PF_6 solution was added until no further precipitation occurred. The suspension was filtered off, and the solid recrystallized from H_2O/acetone to give **15**·4PF_6 as a white solid (550 mg, 82%); mp 228–229 °C; ^{1}H NMR (200 MHz, CD_3CN, 25 °C): δ 9.02, 8.98 (2 × d, J = 7.8, 6.8 Hz, 4H, α-pyr$^+$); 8.42, 8.38 (2 × d, J = 7.2, 6.0 Hz, 4H, β-pyr$^+$); 5.93 (s, 4H, CH_2(T)); 5.83 (s, 4H, CH_2(B)); ^{13}C NMR (50.3 MHz, CD_3CN) δ 151.7, 150.8, 147.0, 146.3, 133.3, 130.8, 130.3, 130.0, 128.2, 128.0, 65.5, 57.2; ESIMS (60 eV): m/z 1024 ([M + 3PF_6]$^+$, 44%), 440 ([M/2]$^{2+}$, 100).

X-Ray crystallography

Data were collected on Siemens P4/PC diffractometers using ω-scans. The structures were solved by direct methods and they were refined based on F^2 using the SHELXTL program system.[18]

Crystal data for 10·4PF$_6$. [$C_{60}H_{69}N_7O_{10}$](PF_6)$_4$·4MeCN, M = 1792.32, triclinic, $P\bar{1}$ (no. 2), a = 13.5888(7), b = 14.7300(10), c = 22.343(2) Å, α = 71.118(5), β = 74.753(5), γ = 78.274(5)°, V = 4048.3(5) Å^3, Z = 2, D_c = 1.470 g cm^{-3}, μ(Cu-Kα) = 1.906 mm^{-1}, T = 203 K, red rhombs; 11 798 independent measured reflections, F^2 refinement, R_1 = 0.071, wR_2 = 0.184, 8887 independent observed reflections [$|F_o| > 4\sigma(|F_o|)$, $2\theta_{max}$ = 120°], 1123 parameters. CCDC 708196.

Crystal data for 11·4PF$_6$. [$C_{56}H_{66}N_{10}O_{10}$](PF_6)$_4$·5MeCN, M = 1824.34, triclinic, $P\bar{1}$ (no. 2), a = 13.5062(6), b = 16.485(2), c = 18.6366(12) Å, α = 98.186(7), β = 92.115(4), γ = 104.056(7)°, V = 3973.1(5) Å^3, Z = 2, D_c = 1.525 g cm^{-3}, μ(Cu-Kα) = 1.968 mm^{-1}, T = 183 K, red prismatic blocks; 13 163 independent measured reflections, F^2 refinement, R_1 = 0.060, wR_2 = 0.149, 10 254 independent observed reflections [$|F_o| > 4\sigma(|F_o|)$, $2\theta_{max}$ = 128°], 1097 parameters. CCDC 708197.

Acknowledgements

This research was financially supported by the *Dirección General de Investigación* (MEC–Spain) through projects CTQ2006-11821/BQU and TEC2008-06883-C03-02 and the *Generalitat de Catalunya* (2005SGR00158). S. R. thanks the *Universitat de Barcelona* for a fellowship.

References

1 C. O. Dietrich-Buchecker, J.-P. Sauvage and J. P. Kintzinger, *Tetrahedron Lett.*, 1983, **24**, 5095–5098.
2 (*a*) C. O. Dietrich-Buchecker and J.-P. Sauvage, *Chem. Rev.*, 1987, **87**, 795–810; (*b*) *Templated Organic Synthesis*, ed. F. Diederich and P. Stang, Wiley-VCH, New York, 2000; (*c*) Templates in Chemistry I, *Top. Curr. Chem.*, ed. C. A. Schalley, F. Vögtle and K. H. Dotz, 2004, vol. 248; (*d*) Templates in Chemistry II, *Top. Curr. Chem.*, ed. C. A. Schalley, F. Vögtle and K. H. Dotz, 2005, vol. 249.
3 *Molecular Catenanes, Rotaxanes and Knots*, ed. J.-P. Sauvage and C. O. Dietrich-Buchecker, Wiley-VCH, Weinheim, 1999.
4 (*a*) *Molecular Devices and Machines*, V. Balzani, A. Credi and M. Venturi, Wiley-VCH, Weinheim, 2nd edn, 2008; (*b*) S. Saha and J. F. Stoddart, *Chem. Soc. Rev.*, 2007, **36**, 77–92; (*c*) M. S. Vickers and P. D. Beer, *Chem. Soc. Rev.*, 2007, **36**, 211–225; (*d*) B. Champin, P. Mobian and J.-P. Sauvage, *Chem. Soc. Rev.*, 2007, **36**, 358–366.
5 K. E. Griffiths and J. F. Stoddart, *Pure Appl. Chem.*, 2008, **80**, 485–506.
6 (*a*) B. L. Feringa, R. A. van Delden, N. Koumura and E. M. Geertsema, *Chem. Rev.*, 2000, **100**, 1789–1816; (*b*) Y. Okada, Z. H. Miao, M. Akiba and J. Nishimura, *Tetrahedron Lett.*, 2006, **47**, 2699–2702.
7 S. A. Vignon and J. F. Stoddart, *Collect. Czech. Chem. Commun.*, 2005, **70**, 1493–1576, and references therein.
8 E. Alcalde, M. Alemany, N. Mesquida, L. Perez-Garcia, S. Ramos and M. L. Rodriguez, *Chem.–Eur. J.*, 2002, 474–484, and references cited therein.
9 E. Alcalde, N. Mesquida and L. Pérez-García, *Eur. J. Org. Chem.*, 2006, 3988–3996.

10 E. Alcalde, L. Pérez-García, S. Ramos, J. F. Stoddart, A. J. P. White and D. J. Williams, *Chem.–Eur. J.*, 2007, **13**, 3964–3979.
11 P. L. Anelli, P. R. Ashton, R. Ballardini, V. Balzani, M. Delgado, M. Gandolfi, T. T. Goodnow, A. E. Kaifer, D. Philp, M. Pietraszkiewicz, L. Prodi, M. V. Reddington, A. M. Z. Slawin, N. Spencer, J. F. Stoddart and D. J. Williams, *J. Am. Chem. Soc.*, 1992, **114**, 193–218.
12 E. Alcalde, C. Ayala, I. Dinarès and N. Mesquida, *J. Org. Chem.*, 2001, **66**, 2291–2295.
13 D. B. Amabilino, P. R. Ashton, M. S. Tolley, J. F. Stoddart and D. J. Williams, *Angew. Chem., Int. Ed. Engl.*, 1993, **32**, 1297–1301.
14 E. Alcalde, L. Pérez-García, C. Miravitlles, J. Rius and E. Valentí, *J. Org. Chem.*, 1992, **57**, 4829–4834.
15 This type of interaction has been observed previously, see: (*a*) P. N. Jagg, P. F. Kelly, H. S. Rzepa, D. J. Williams, J. D. Woollins and W. Wylie, *J. Chem. Soc., Chem. Commun.*, 1991, 942–944; (*b*) V. C. Gibson, C. Newton, C. Redshaw, G. A. Solan, A. J. P. White and D. J. Williams, *Eur. J. Inorg. Chem.*, 2001, 1895–1903.
16 D. B. Amabilino, P. L. Anelli, P. R. Ashton, G. R. Brown, E. Córdova, L. A. Godínez, W. Hayes, A. E. Kaifer, D. Philp, A. M. Z. Slawin, N. Spencer, J. F. Stoddart, M. S. Tolley and D. J. Williams, *J. Am. Chem. Soc.*, 1995, **117**, 11142–11170.
17 D. D. Perrin and L. F. Armarego, *Purification of Laboratory Chemicals*, Pergamon Press, 2nd edn, 1980.
18 *SHELXTL PC version 5.03*, Siemens Analytical X-Ray Instruments, Inc., Madison, WI, 1994; *SHELXTL PC version 5.1*, Bruker AXS, Madison, WI, 1997.